

Universität Tübingen

Bachelor
Geowissenschaften
Umweltnaturwissenschaften

Modul
GEOPHYSICS 1&2

Course Notes

for use in this lecture only

(figures are partly taken from books and journals but not explicitly cited for simplicity)

Erwin Appel
2013/2014

A Introduction

See Part I

B Gravimetry

See Part I

C Magnetics

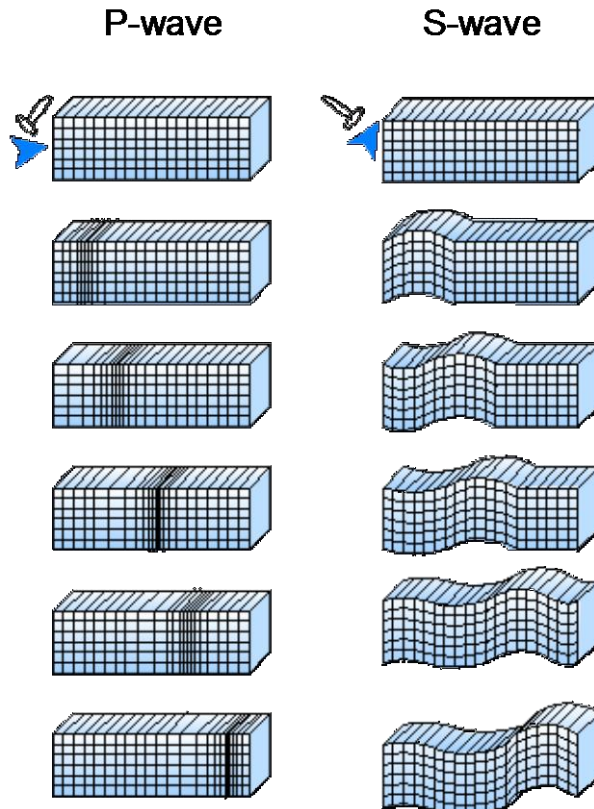
See Part I

D Electrics and Electromagnetics

See Part I

E Seismics & seismology

E.1 Seismic wave types



velocities

p - wave

$$v = \sqrt{\frac{K + \frac{4}{3}\mu}{\rho}}$$

s - wave

$$v = \sqrt{\frac{\mu}{\rho}}$$

Characteristics of displacement for p- and s-waves (body waves)

p-wave: displacement u_x parallel to propagation direction (x)

s-wave: displacement u_z perpendicular to propagation direction (x)

K - bulk modulus: $\tau = K \cdot \Delta V/V$ (τ : hydrostatic pressure; $\Delta V/V$: relative volume change)

μ - shear modulus: $\sigma = \mu \cdot \phi$ (σ : shear stress; ϕ : shear angle)

ρ : density

Wave equation:

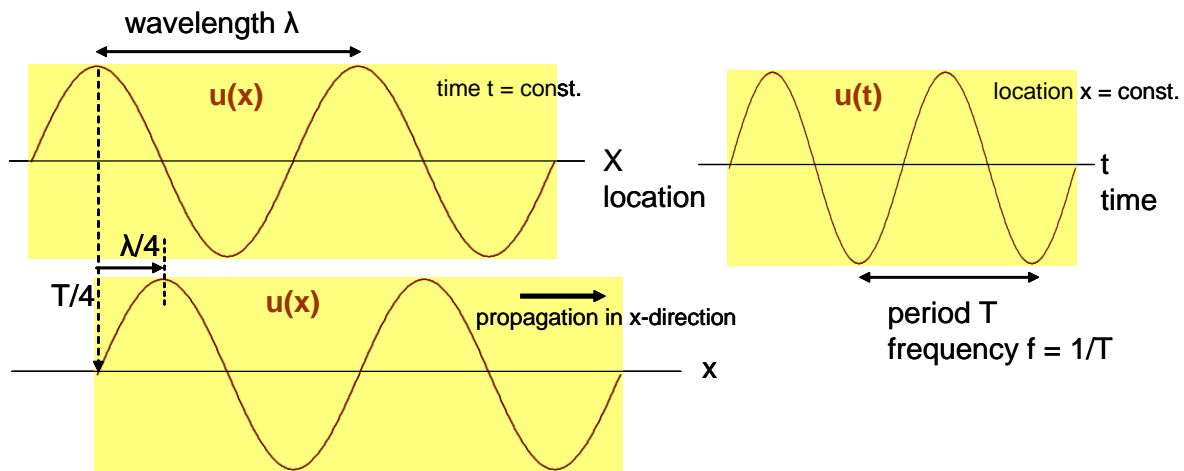
p-wave
$$\frac{\partial^2 u_x}{\partial t^2} = v^2 \frac{\partial^2 u_x}{\partial x^2}$$

s-wave
$$\frac{\partial^2 u_z}{\partial t^2} = v^2 \frac{\partial^2 u_z}{\partial x^2}$$

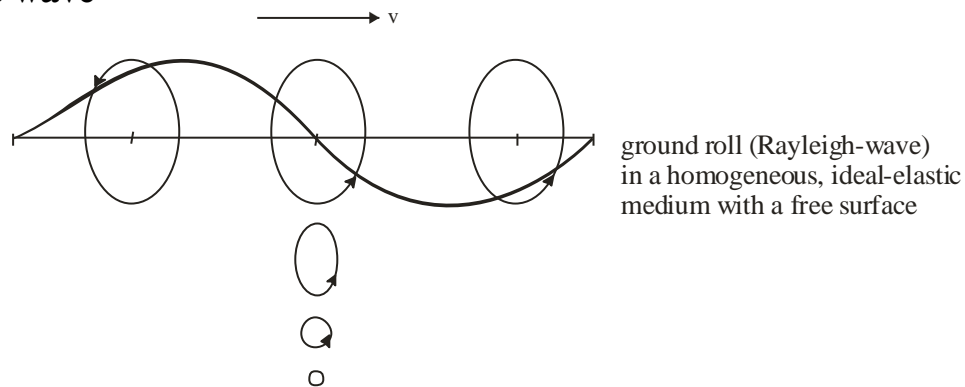
Solution of the wave equation:

$$u_x(x, t) = u_{x0} \cdot \sin(k \cdot x - \omega \cdot t)$$

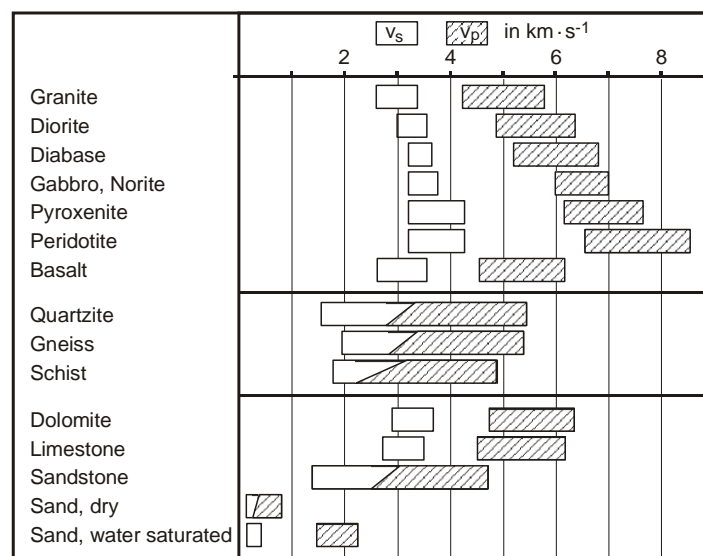
$$u_z(x, t) = u_{z0} \cdot \sin(k \cdot x - \omega \cdot t)$$

Explanation of phase velocity v , wavelength λ , period T , frequency $f=(1/T)$:

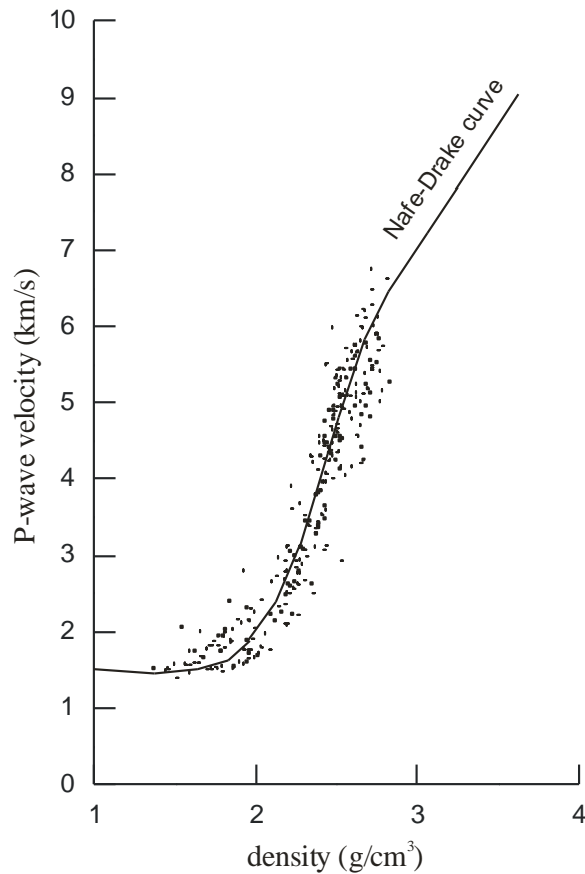
Wave propagates with velocity $v = (\lambda/4)/(T/4)$, and therefore $v = \lambda / T$ or $v = \lambda \cdot f$

Surface wave

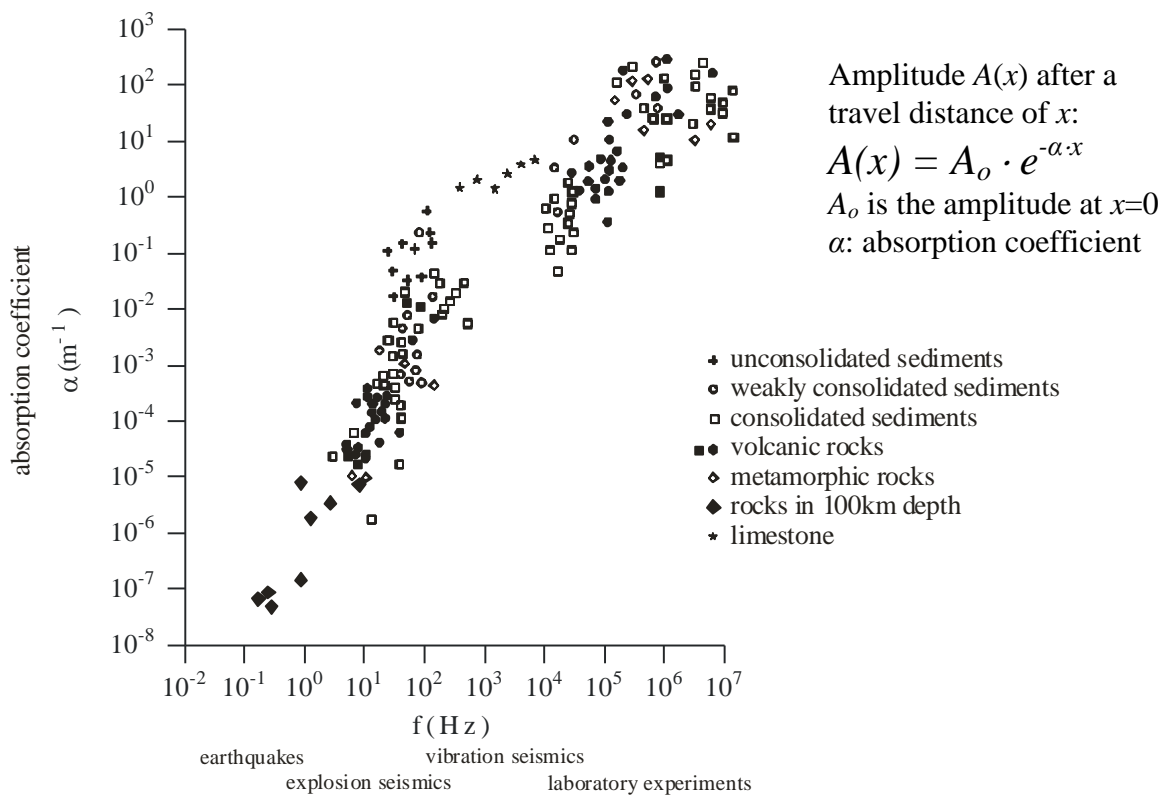
The Rayleigh wave shows an elliptical movement of the dislocation (similar to water wave, but with dislocation moving anticlockwise, instead of clockwise as for water waves). The amplitude of dislocation decreases with depth and it becomes more circular.

E.2 Velocities

Mean-value range of longitudinal and transverse wave velocities



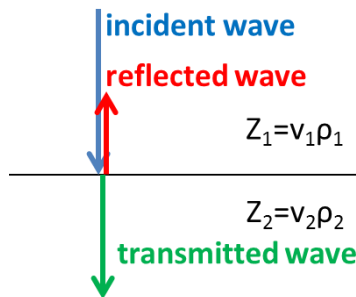
P-wave velocity increases as a function of density; this relationship is very good for ideal elastic (high density), fairly good for rocks with intermediate density, and quite weak to very weak in low density unconsolidated sediments



The absorption coefficient α rapidly increases with frequency, and absorption is also dependent on the rock properties (compare the much higher absorption in less consolidated sediments compared to consolidated sediments around 100 Hz).

E.3 Waves at boundaries and Huygens' principle

Refraction and reflection



For vertical angle of incidence we get:

$$R = \frac{Z_1 - Z_2}{Z_1 + Z_2}; \quad D = \frac{2Z_{12}}{Z_1 + Z_2}; \quad Z = v \cdot \rho \text{ acoustic impedance}$$

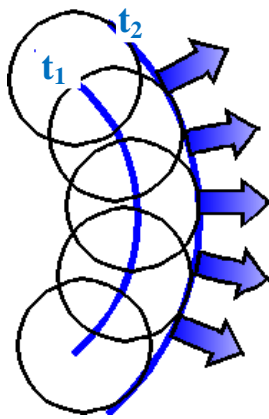
R: reflection coefficient

amplitude ratio of reflected wave and incident wave

D: transmission coefficient

amplitude ratio of transmitted wave and incident wave

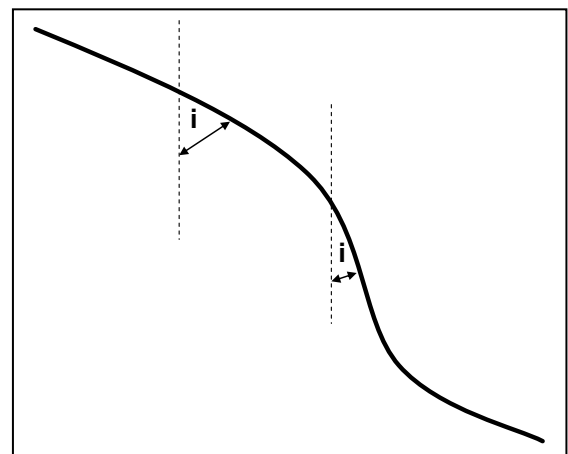
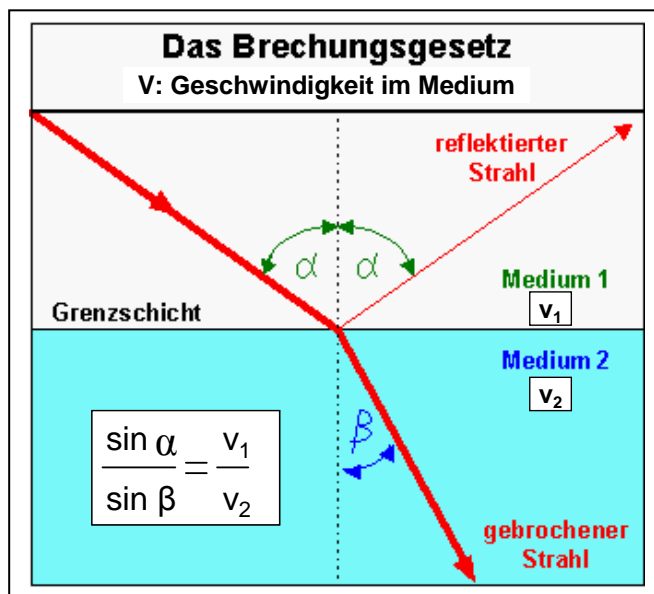
Huygens' principle



Each point on a wavefront (here the wavefront at the time t_1) acts as the center of an elementary wave (spherical waves). Within a given time increment Δt the elementary waves travel a distance of $v \cdot \Delta t$ (v is the velocity in that region). The new wavefront at the time $t_2 = t_1 + \Delta t$ is given by the envelope of the elementary waves.

With the Huygens principle one can do forward modelling of ray propagation (for a given spatial velocity distribution – even a complex one)

From the Huygens principle we derive the reflection and refraction laws:



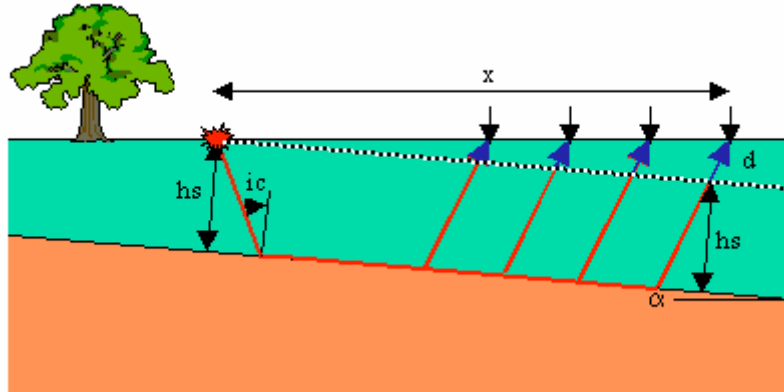
Other formulation of the refraction law:
 $\sin(i)/v = p$; p is constant along ray path
 (p : ray parameter)

With the general refraction law “ $\sin(i)/v = p$ constant”, one can also do forward modelling of ray propagation, based on a given velocity spatial model (one starts with a certain direction for the ray path at one point and keeps $\sin(i)/v$ constant along the ray path).

Waves with oblique incidence create converted waves: $P \rightarrow SV$; $SV \rightarrow P$ (for SH no conversion)
 “V” and “H” indicate vertical and horizontal polarization (in respect to the layer boundary)

Head wave (see also separate ppt File)

An incident wave with the critical angle of incidence i_c is refracted under the angle of 90° (when $v_2 > v_1$). It travels along (below) the interface with the velocity v_2 . All along its travel path a head wave is emerging travelling upward under the angle i_c .

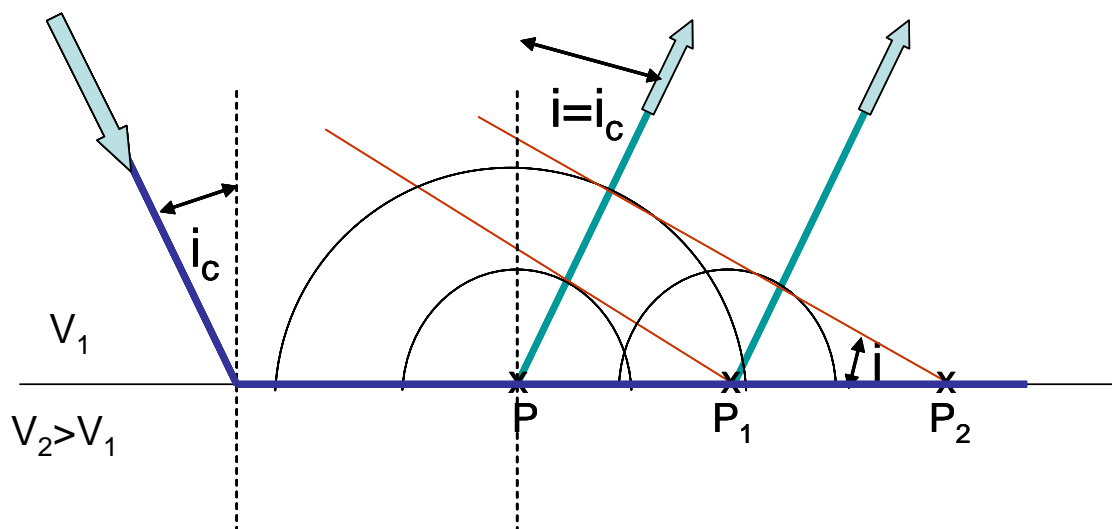


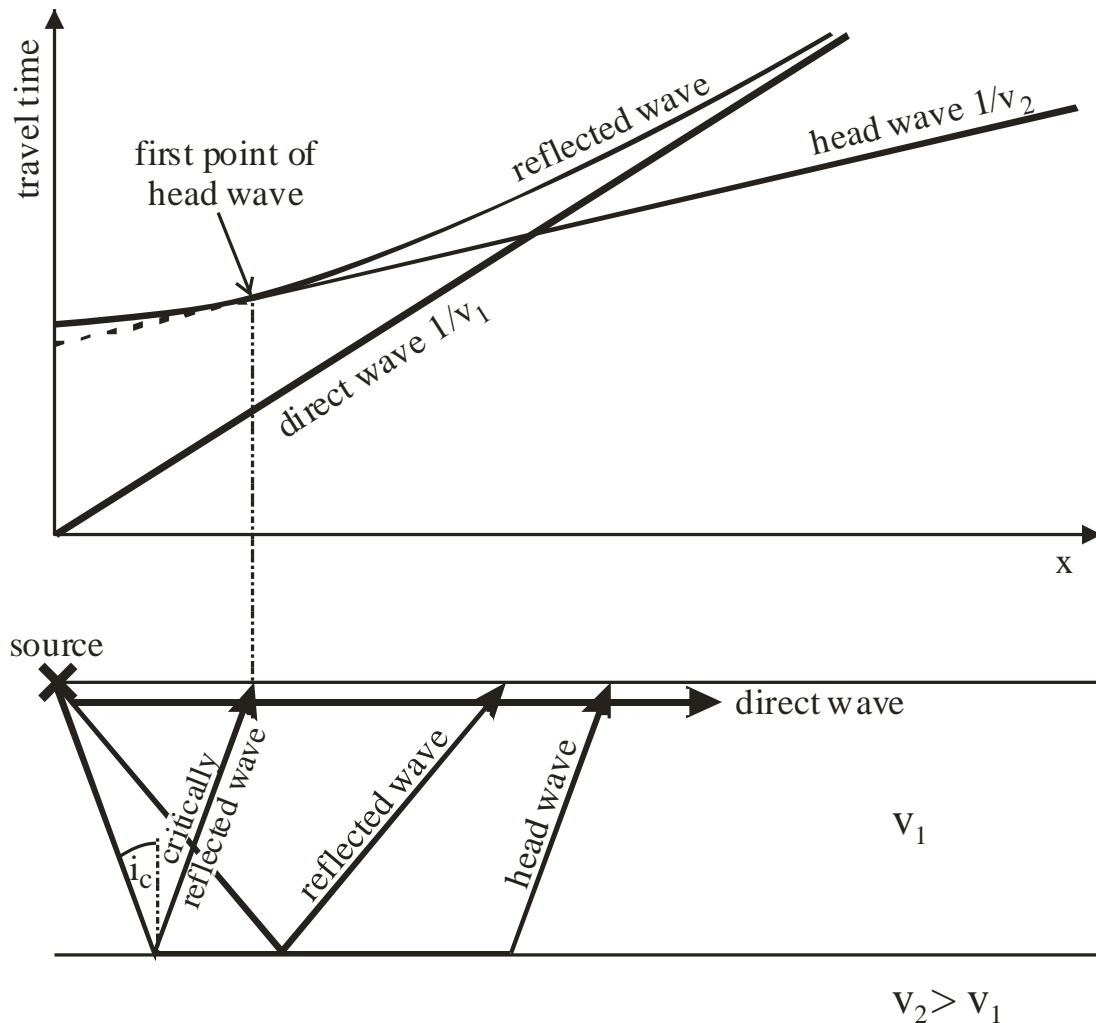
The existence of the head wave can be explained by Huygens' Principle: Consider an arbitrary point P at the interface along the travel path of the critically refracted wave. The critically refracted wave passes through P at a time t .

At the time $t + \Delta t$ the critically refracted wave has advanced to P_1 whereas an elementary wave emanated from P upward has reached somewhere on the circle with a radius $v_1 \cdot \Delta t$. The resulting wavefront of the up-going wave is the tangent at this circle through P_1 and the ray path is perpendicular to it (head wave).

At the time $t + 2\Delta t$ the elementary wave emanated from P has reached on the circle around P with radius $2v_1 \cdot \Delta t$, at the same time on the circle around P_1 with radius $v_1 \cdot \Delta t$, and also passes through the point P_2 (the point where the critically refracted wave reached at $t + \Delta t$). Thus the wavefront of the upward traveling head wave is the tangent at these two circles (envelope) through the P_2 .

The ray paths of the head wave are all parallel (for constant velocity v_1) and emerge at the angle $i = i_c$. This can be seen by considering the indicated rectangular triangle where $\sin(i) = v_1 \cdot \Delta t / (v_2 \cdot \Delta t) = v_1 / v_2 = \sin(i_c)$.



E.4 Ray paths and travel times

Sketch of ray paths for a two-layer subsurface and related arrival times in a traveltime diagram (we only consider the fastest body waves, i.e. P-wave); the “critically reflected wave” is identical with the head wave nearest to the source

Traveltime equations:

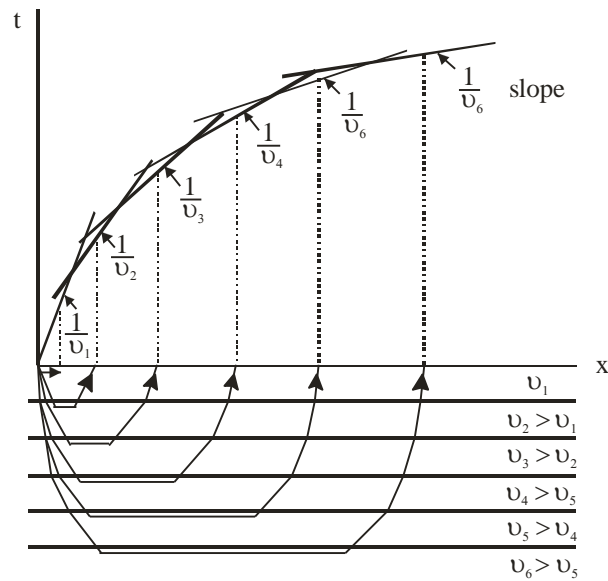
(h : thickness of the top layer)

Direct wave: $t(x) = \frac{1}{v_1} \cdot x$ linear function (slope $1/v_1$)

Reflected wave: $t(x) = \frac{1}{v_1} \cdot \sqrt{x^2 + (2h)^2}$ hyperbola function

Head wave: $t(x) = \frac{1}{v_2} \cdot x + \frac{2h \cdot \cos(i_c)}{v_1}$ linear function (slope $1/v_2$)

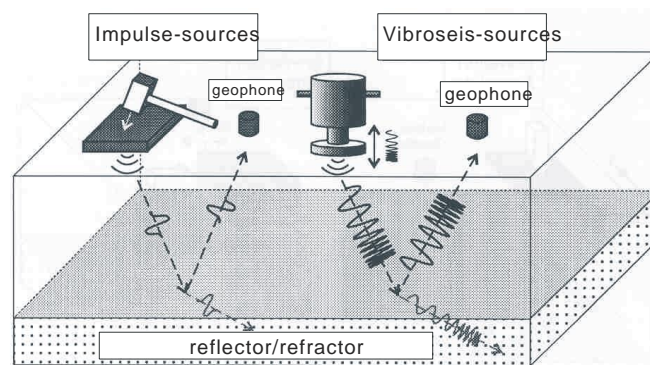
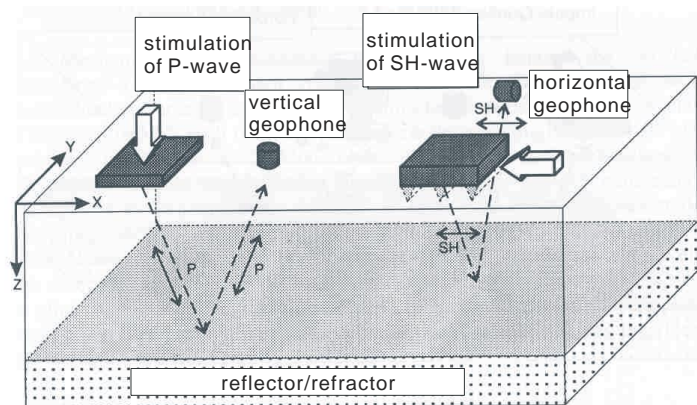
- In near distance to the shot point the direct wave makes the first arrival
- In far distance to the shot point the head wave makes the first arrival
- The reflected approximates to the direct wave for large distances, but never makes first arrivals
- The head wave first occurs at a certain distance from the shot point; the traveltime at this point is identical to the reflected wave; the extrapolation of the head wave curve to the shot point gives the intercept time $t_i = 2h \cos(i_c) / v_1$



Traveltime curve of head waves for horizontal layering (multiple layers) – a continuous increase of velocity with depth produces a traveltime curve with a decreasing slope; the ray paths are bent and the slope of the traveltime curve at a point P gives the velocity at the deepest point of that bent ray path which reaches the surface at P

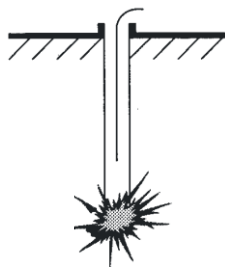
E.5 Principles of seismic measurements

Seismic sources

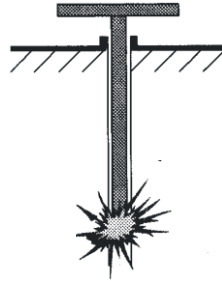


(top) Creating P waves and S waves

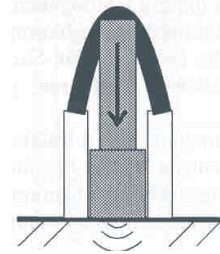
(bottom) Impulse and vibration sources (hydraulic or electrodynamic vibrators)



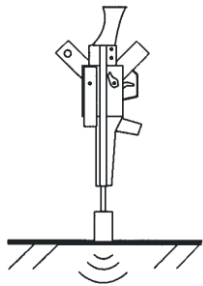
explosive



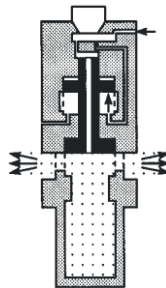
shot pipe



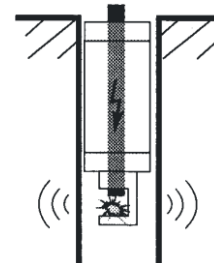
accelerated weight dropper



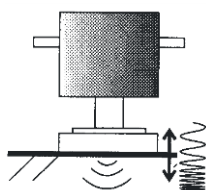
modified gun



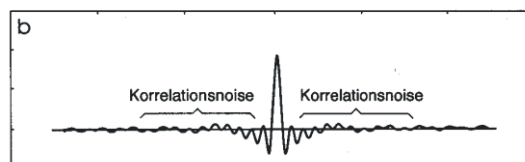
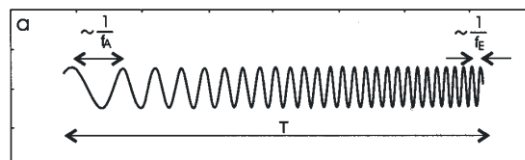
airgun



sparker



vibrator



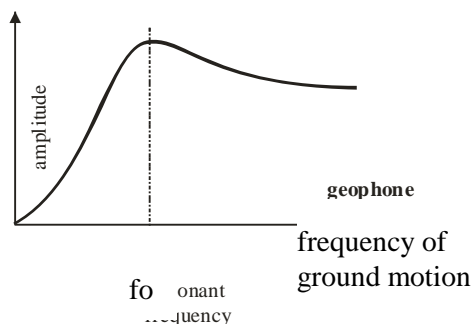
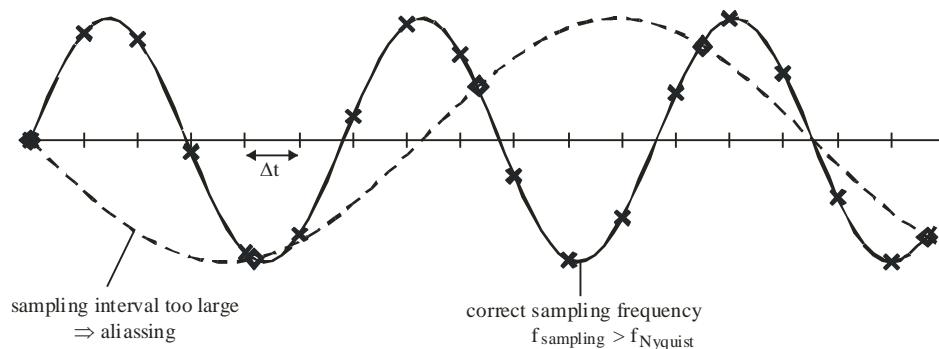
Seismic Sources for P-waves are manifold

Data acquisition

Seismic recording is usually digital recording. The analogue signal from seismometers (which is usually a voltage) is converted into digital values (obtained at a certain sampling rate Δt)

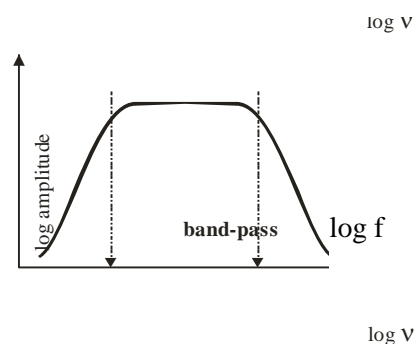
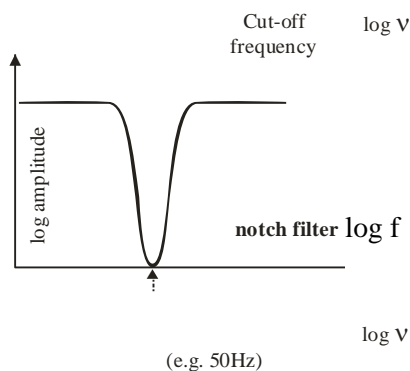
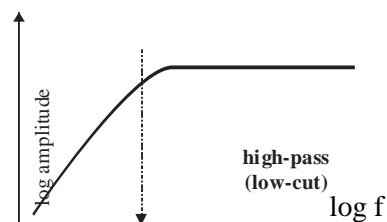
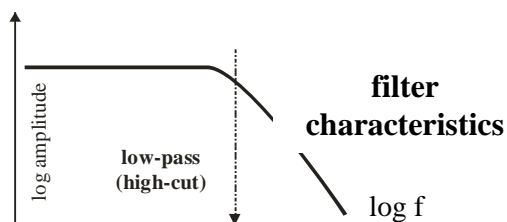
Some main important issues for data acquisition are

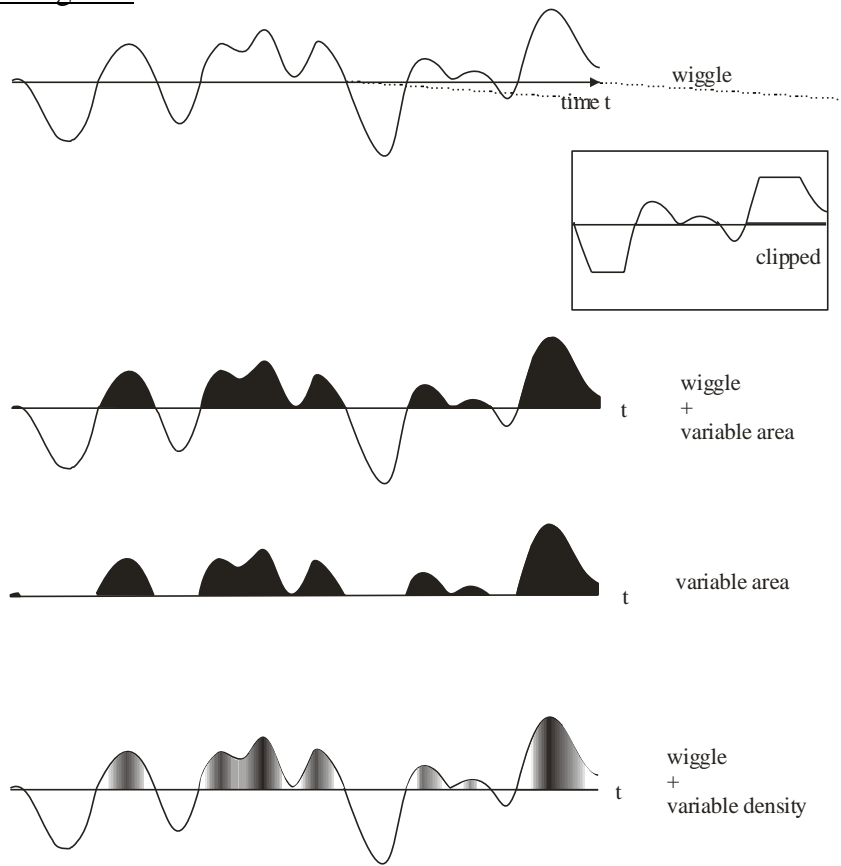
- filtering (analogue and digital filters)
 - Amplitude ratios are often given in dB: value in dB = $20 \log (A_1/A_2)$
- aliasing (if $\Delta t > \text{Nyquist interval}$, then the frequency in the digital seismogram will be different from the frequency in the original analogue seismogram)



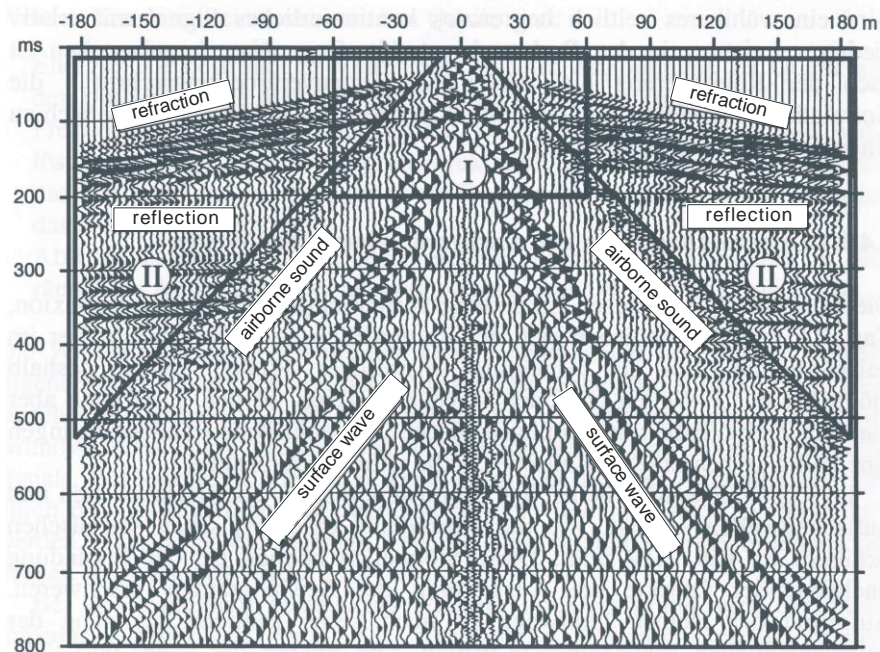
frequency characteristic of a seismometer

the seismometer works as a low-cut filter



Plotting of seismograms

Different ways of plotting seismic signals

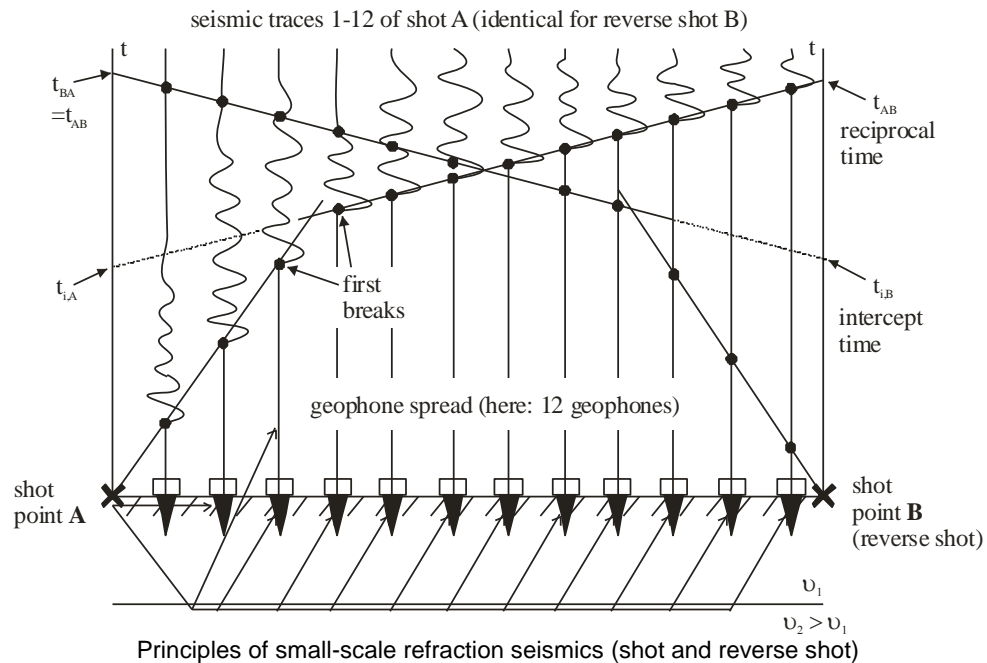


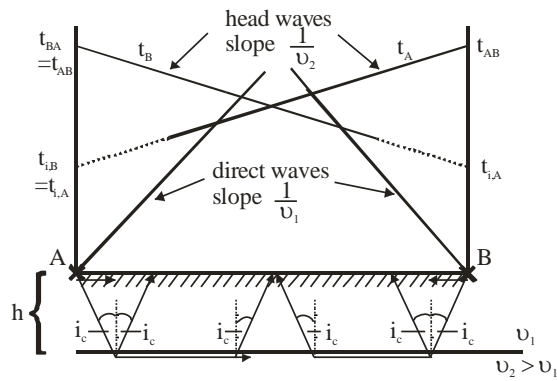
I: window of near surface investigation

II: window with a good signal/noise-ratio

Example for the record of a seismic shot (seismic traces plotted as wiggle + variable area) showing different signals with different arrival times

E.6 Refraction seismics

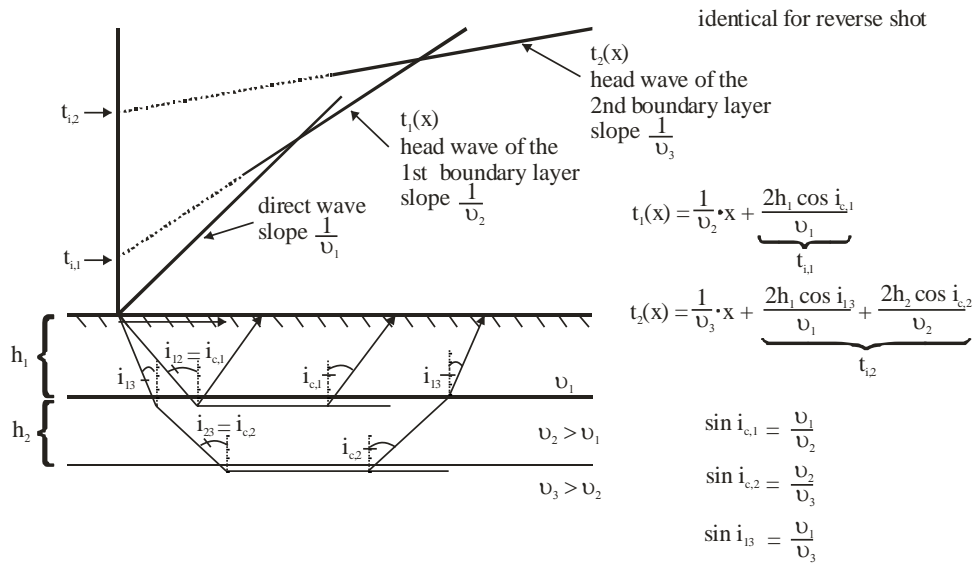




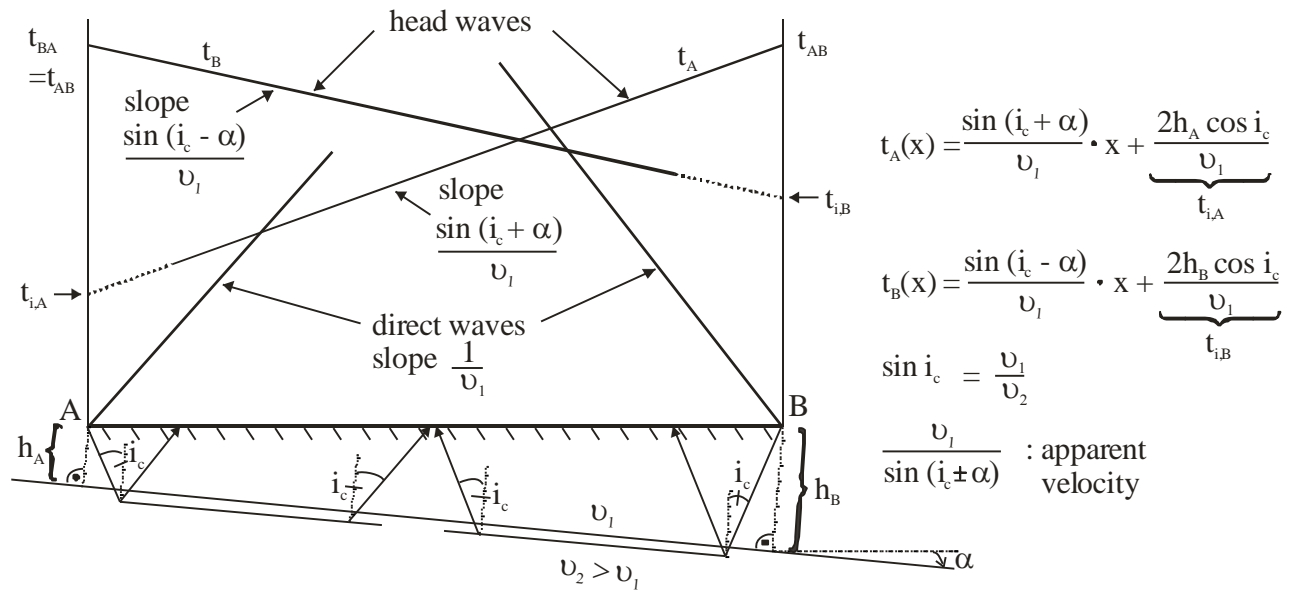
$$t(x) = t_A(x) = t_B(x) = \frac{1}{v_2} \cdot x + \underbrace{\frac{2h_1 \cos i_c}{v_1}}_{t_{iA} = t_{iB}}$$

x : distance source to geophone

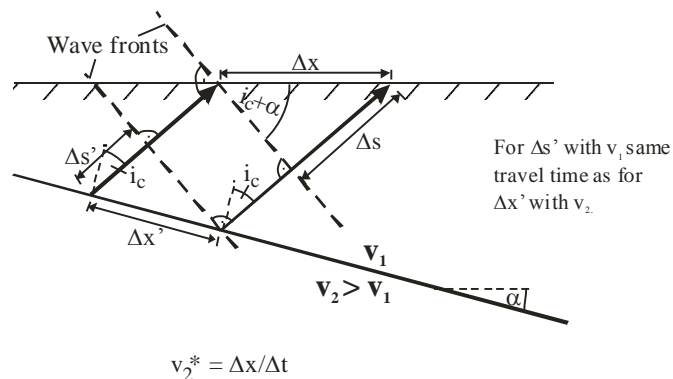
$$\sin i_c = \frac{v_1}{v_2}$$



Inversion of traveltime curves for two and three horizontal layers



Apparent velocity v_2^* :



Inversion of traveltime curves for a two-layer case with inclined layer boundary – the velocity determined from the slope of the traveltime curve represents an apparent velocity.

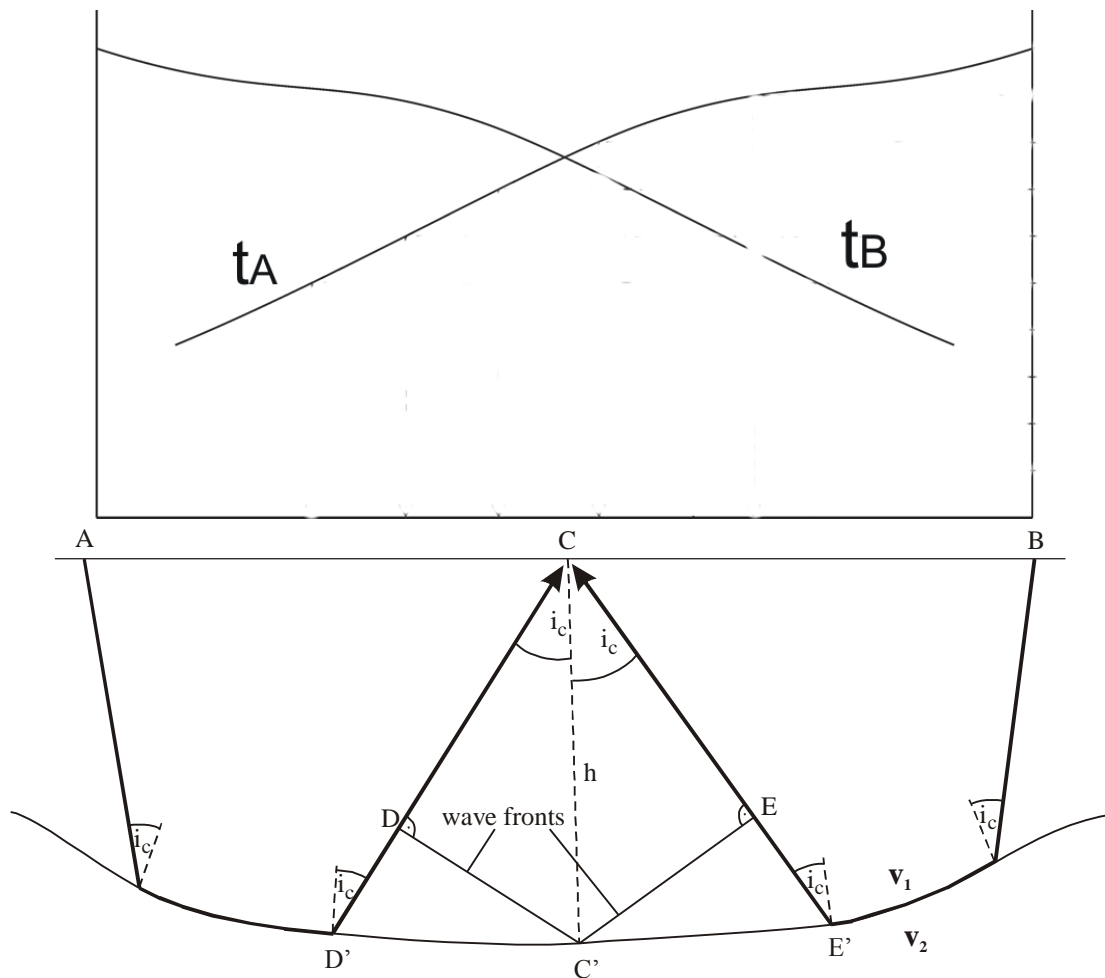
For **curved layer boundaries**, the intercept time method cannot be used. Instead there is a variety of other methods. The simplest one is the **Plus-Minus Method**, which requires a combination of traveltime curves from shot and reverse shot.

Here the traveltimes t_{AC} and t_{BC} at the same point (C) are combined into the so-called plus-time t_+ and the minus-time t_- . Using all possible points C results in a t_+ curve and a t_- curve.

The average slope of the t_- curve gives the velocity v_2 below the layer boundary.

The t_+ curve represents information about the depth of the boundary.

The principles of the Plus-Minus method are outlined below.



The traveltime from D' to D (with velocity v_1) is equal to the traveltime from D' to C' (with velocity v_2)
 The traveltime from E' to E (with velocity v_1) is equal to the traveltime from E' to C' (with velocity v_2)

Therefore: $t_{AC} = t_{AC'} + t_{DC}$ and $t_{BC} = t_{BC'} + t_{EC}$ with $t_{DC} \approx t_{EC} \approx h \cos(i_c)/v_1$

Forming $t_{AC} + t_{BC} = t_{AC'} + t_{BC'} + 2h \cos(i_c)/v_1$

As $t_{AC} + t_{BC} = t_{AB}$ we get:

$$t_{AC} + t_{BC} - t_{AB} =: t_+ = 2h \cos(i_c)/v_1 \quad \text{plus-time}$$

$$\text{and } (t_{AC} - t_{BC} + t_{AB})/2 =: t_- \quad \text{minus-time}$$

t_{AC} , t_{BC} , t_{AB} are taken from the measured traveltime curves at the same profile points.

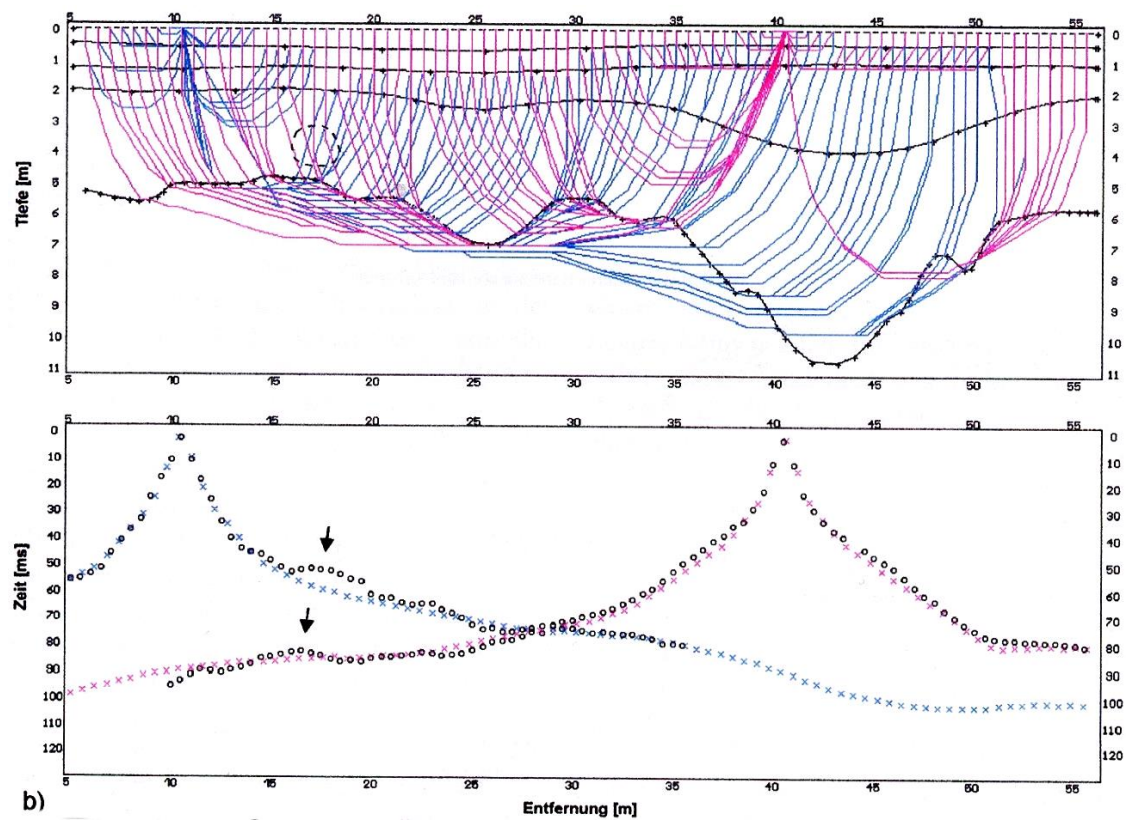
After determining v_2 from the minus-time curve, one can calculate i_c and then $h = \frac{t_+ \cdot v_1}{2 \cos(i_c)}$

The Plus-Minus method is an approximate method as the rays from shots A and B arriving at the same point C at surface do not originate at the same points at the boundary. Therefore there is an averaging effect for the segment between these foot points D' and E' leading to a smoothing of the curvature of the determined boundary and an averaging of possible velocity changes of v_2 along the boundary.

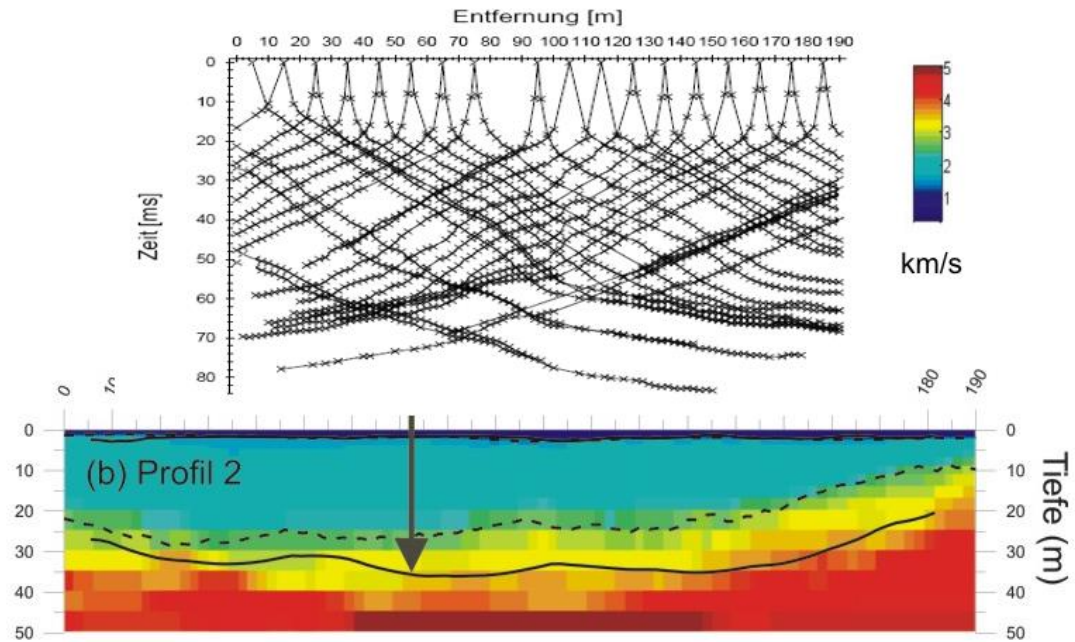
The **Generalized Reciprocal Method (GRM)** is an improvement of the Plus-Minus method. It combines traveltimes of shot and reverse shot for rays which originate from the same point at the boundary. The GRM allows also determining variation of v_2 along the boundary.

Some further advanced methods for inverting refraction seismic data are the **Wavefront Method** and the **CMP Method**. With densely distributed shot points one can perform a **Refraction Tomography** that yields the velocity variation within layers.

For complicated structures **Ray Tracing** can improve the results. Some examples follow below.



Example for applying GRM and subsequent ray tracing (doline structure "Schwäbische Alb").



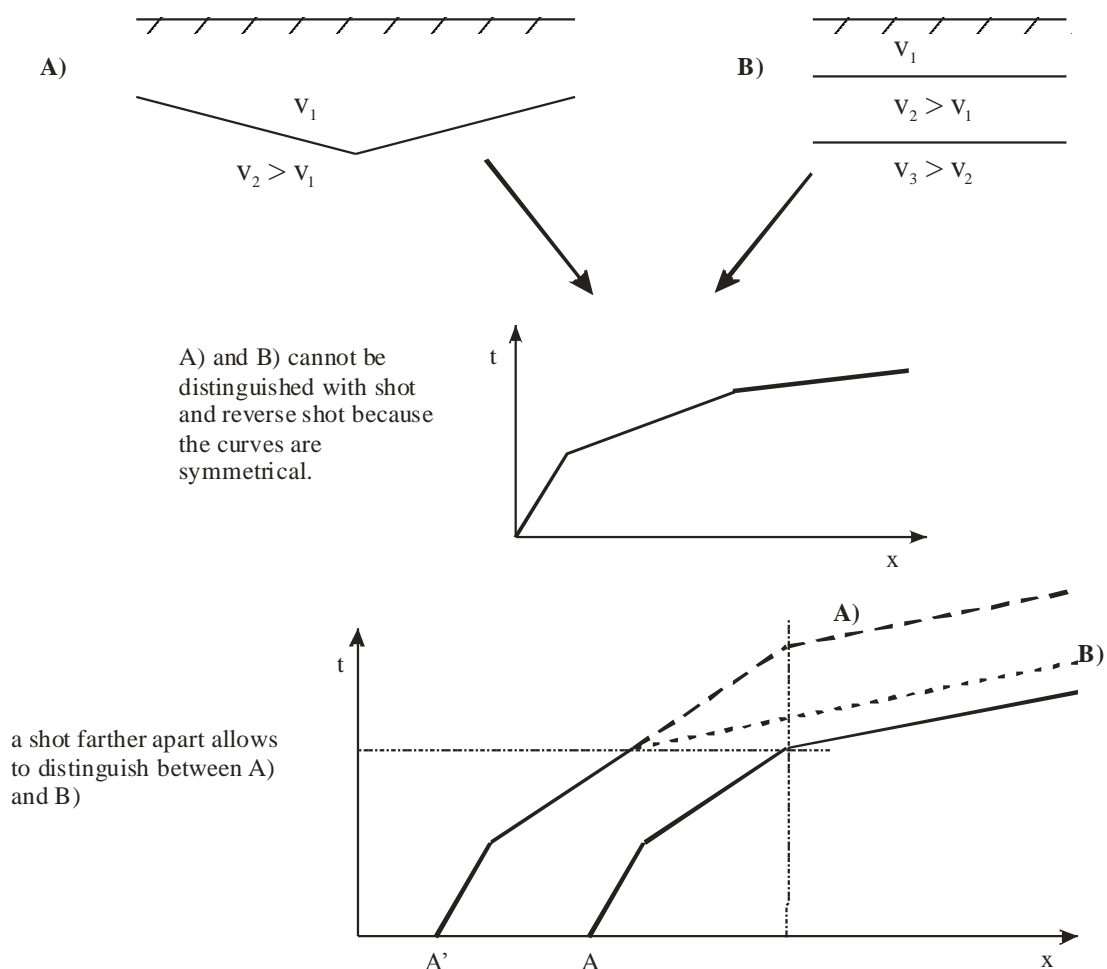
Example for refraction tomography (valley fill on limestone bedrock near the "Blautopf" at Blaubeuren)

Problems in refraction seismics

Multiple layer or lateral change?

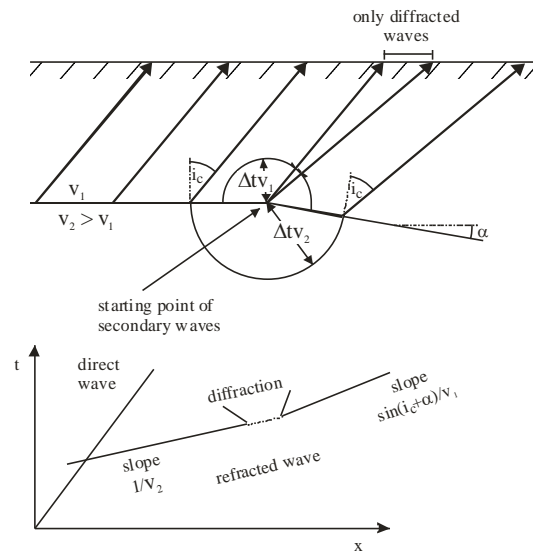
A crucial task before starting data inversion is to assign segments of the first arrival traveltime curve to head waves from certain layers. A change in the slope of the traveltime curve can mean that a head wave from a deeper boundary overtakes the head wave of a shallower boundary, but alternatively it can also mean that the dip of the boundary is changing (or also the velocity below the boundary may change). The operator has to decide what is true – for this one needs traveltime curves from shot and reverse shot but also far-end shots. This is illustrated below.

The traveltime curve from a boundary changing from down-dipping to up-dipping can be not distinguished from a horizontal 3-layer case. When the structure is symmetric also the traveltime curve of the reverse shot is identical. A far-end shot is needed to distinguish in between the two possibilities.



If there is a change in the slope of the boundary, the point where it appears in the traveltime curve remains at the same location when the shot point is moved from A to A'.

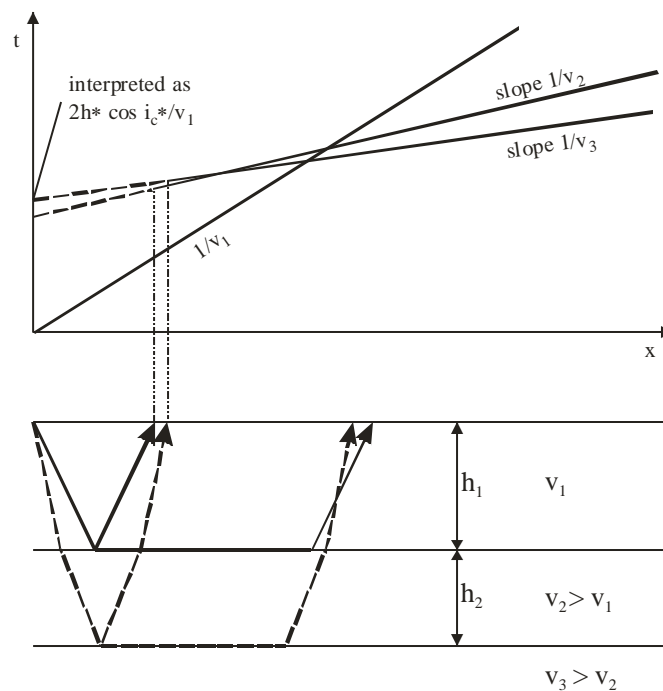
If there is a second head wave overtaking the first one, then the point where the slope changes moves with the shot point.



A boundary changing from up-dipping (or horizontal) to down-dipping cannot be misinterpreted as a 3-layer case

Hidden layer (see also separate ppt File)

Hidden layers are a major problem in shallow refraction seismics leading to underestimation of the depth of layer boundaries.

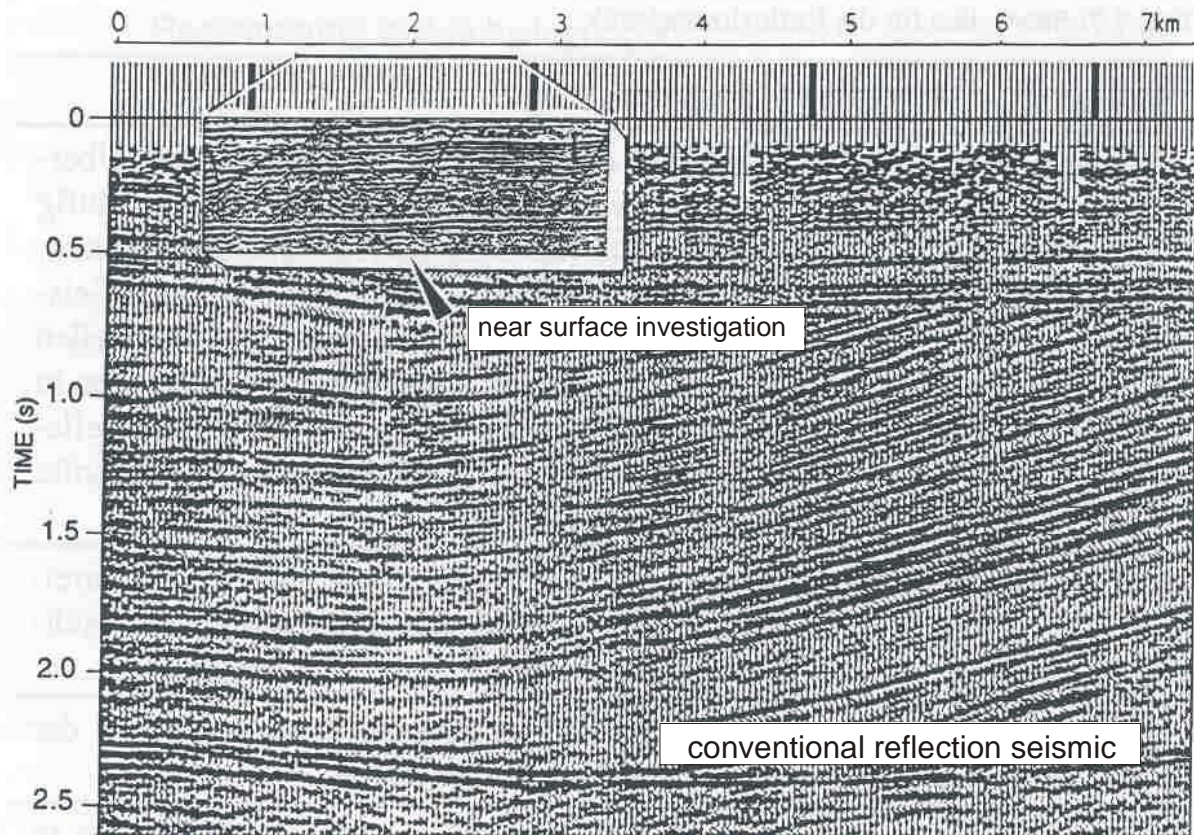


⇒ **determination of an apparent depth h^* for the upper boundary of the v_3 -layer with $h^* < h_1 + h_2$**

Illustration of traveltimes curves for a hidden layer case.

The hidden layer problem is a very common problem in shallow refraction surveys. It is because in a layer of unconsolidated sediments we have a gradual increase of velocities with depth. In the traveltime curve we only see the velocity at the top of the layer.

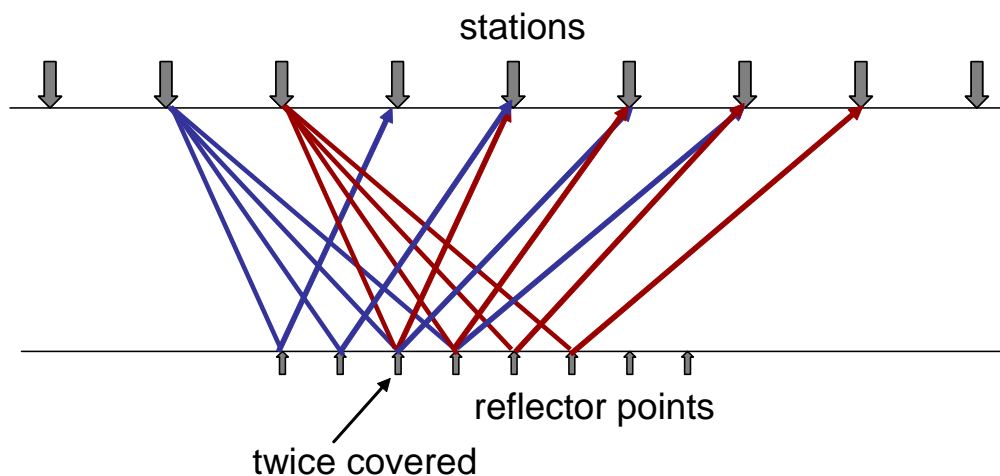
E.7 Reflection seismics



Reflection seismic result: Each seismogram denotes shot and receiver at the same surface location; reflections with high amplitudes are seen as black "lines" (variable area plots)

Data acquisition

Reflection seismic data are usually acquired as common-shot point (CSP) data sets (one shot point and a certain number of recording stations).



Principle of common shot point (CSP) data acquisition in reflection seismics. By multi-channel recording one gets a multi-coverage of reflector points (with N channels the maximum coverage is $N/2$) – in the example the number of channels is 4, the station spacing is 1, and the offset is 2 (number of stations from the shot to the first receiver).

Reducing surface waves

Reflected waves never make first arrivals. Surface waves are a general problem in reflection seismics as they have high amplitudes and can hide reflected signals. To suppress surface waves one can use stacked seismograms from geophone groups (geophones set ca. within a range of one wavelength of the surface wave).

Data processing

Static correction:

Correction of topography (correction to a reference level) and influence of the low velocity surface layer.

Gain adjustment:

With larger traveltime amplitudes become lower because of longer travel path (absorption). This means the amplitudes have to more amplified for longer traveltimes.

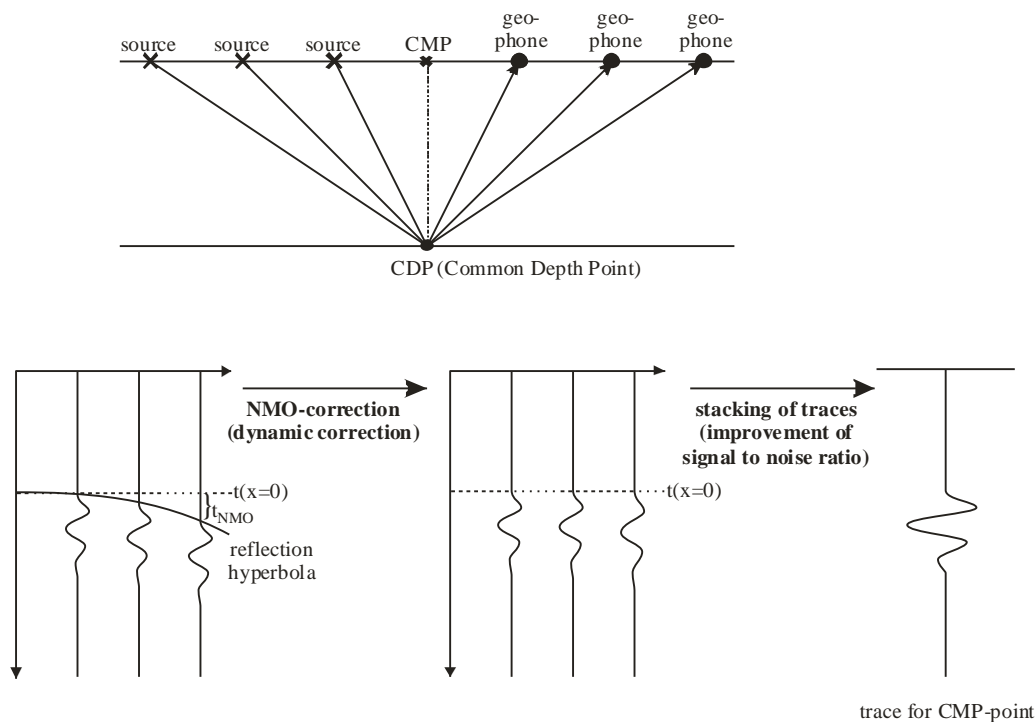
Deconvolution:

Seismic signal is distorted (convoluted) by diffraction and dispersion (e.g. a short wavelet of an explosive source will become longer with along the travel path). The back-projection to a clearer (shorter) signal is called deconvolution.

A similar effect is given when using a vibration source – the original known vibration signal (several seconds long) is used to transform the measured seismogram into a resulting seismogram with short impulse for the wavelet (“spike” deconvolution).

Normal moveout (NMO) correction (dynamic correction) and stacked seismogram:

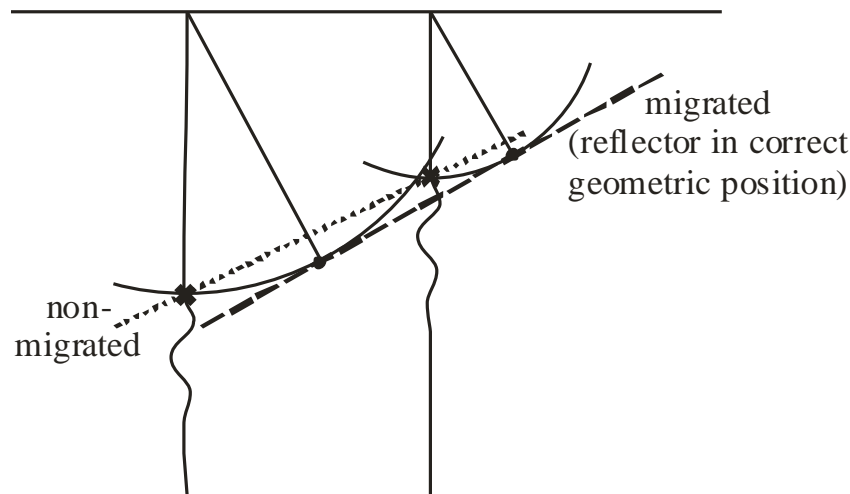
The acquired seismograms are resorted to common mid points (CMP), i.e. combining all traces with the same reflector point. After NMO correction (correcting the reflection hyperbola to same onset time) all traces of a CMP-dataset are stacked. This stacking of multi-covered reflector points enhances the signal-to-noise ratio.



The stacked traces of neighbouring CMPs are plotted next to each other resulting in the final (unmigrated) reflection seismogram as shown in the first image of chapter F.7.

Migration:

After the process described above the reflection seismogram does not show the reflector elements in a correct geometric position (unmigrated reflection seismogram). Transforming the seismogram into a geometrically correct image of reflector elements is called **migration**.



Concept of migration: repositioning of reflector elements
In this sketch the vertical axis is a depth axis (not a traveltime axis): horizontal and vertical scales are equal

Resolution**Vertical resolution**

Two subsequent reflections can be distinguished when their arrival time is at least ca. half a period shifted (note: this definition is not a strict criterion). Consequently the distance between two reflectors must be at least $\frac{1}{4}$ of a wavelength.

e.g. $v=4$ km/s, $f=50$ Hz $\rightarrow \lambda=v/f=80$ m \rightarrow minimum distance of reflectors 20 m
(case of hydrocarbon exploration)

e.g. $v=2$ km/s, $f=100$ Hz $\rightarrow \lambda=v/f=20$ m \rightarrow minimum distance of reflectors 5 m
(case of hydrogeology)

Lateral resolution

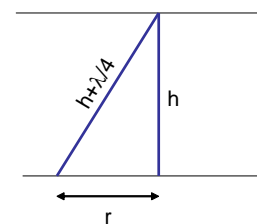
The lateral resolution is given by the radius r of the first Fresnel zone.

$$r = \sqrt{\lambda^2 / 16 + \lambda \cdot h / 2}$$

e.g. $v=4$ km/s, $f=50$ Hz $\rightarrow \lambda=v/f=80$ m, $h=1$ km $\rightarrow r \approx 200$ m
(case of hydrocarbon exploration)

e.g. $v=2$ km/s, $f=100$ Hz $\rightarrow \lambda=v/f=20$ m, $h=10$ m $\rightarrow r \approx 10$ m
(case of hydrogeology)

The values represent the lateral distance of reflector changes to allow correct geometrical imaging. However, shorter-distance variations can be recognized (compare images in the microscope when approaching the optical resolution)

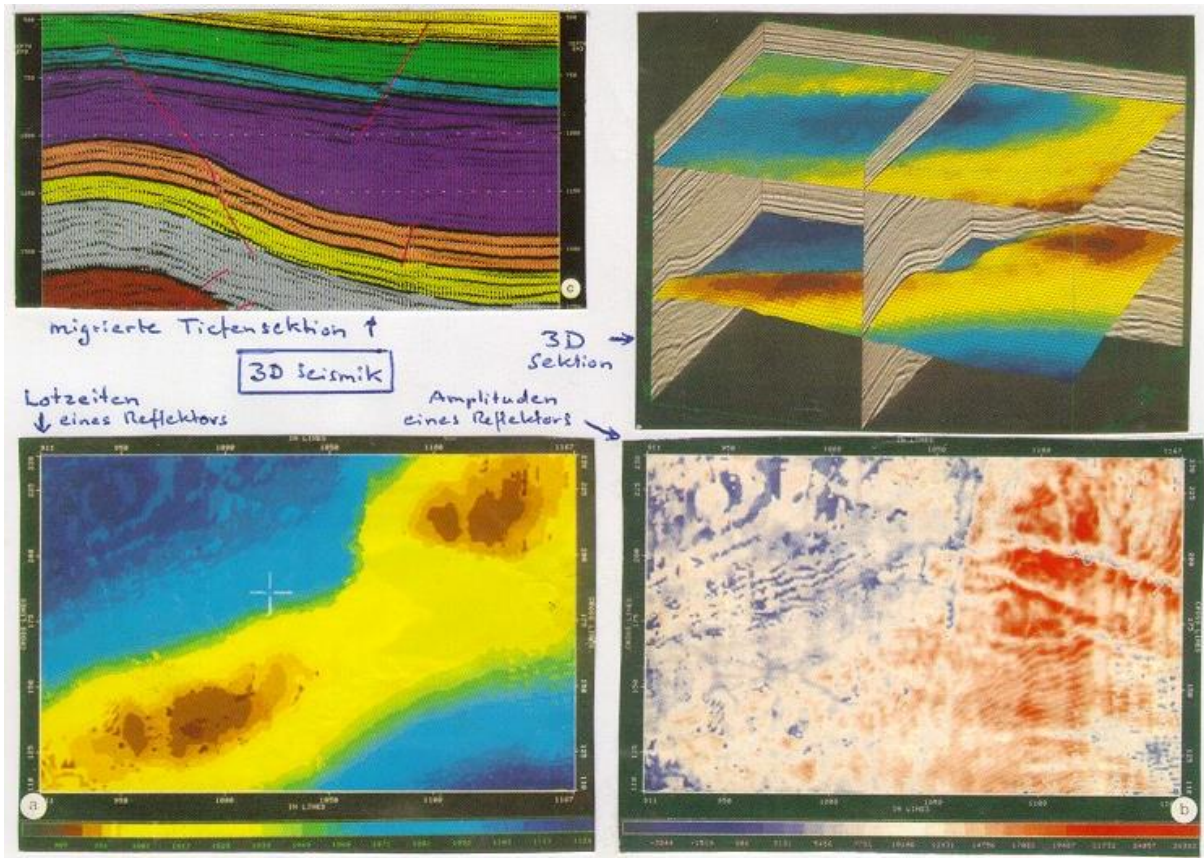
**Shallow subsurface reflection seismics**

The quality of shallow subsurface reflection seismics is limited because

- of the problem to suppress surface waves: geophone groups cannot be applied because the station distance is must smaller than the extent of a geophone group – only reduction of surface waves by high-pass filters is possible (surface waves have lower frequencies than body waves)
- the wavelet is rather long compared to the record length

3D reflection seismics

The principles of 3D seismics, in data acquisition and data processing, are equivalent to 2D seismics. CSP data sets are acquired (shots and receiver line perpendicular to each other), sorting to CMP data sets leads to hyperboloids instead of hyperboles, NMO correction and migration works similar.

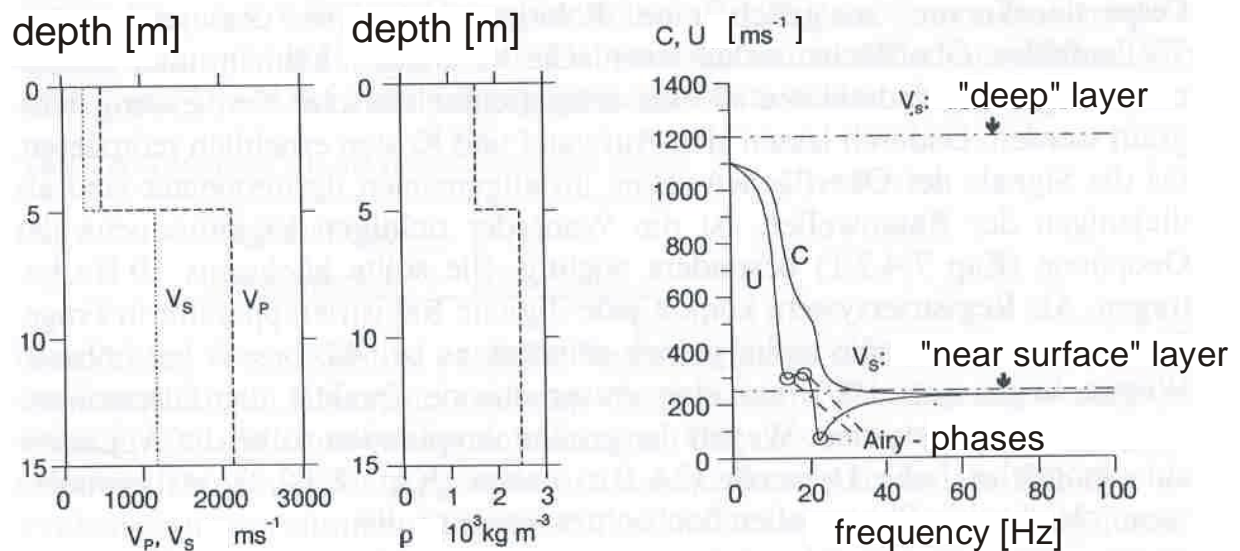


Top row: (left) 2D-seismics result with colour coding for interpreted layers, (right) 3D-seismics result with spatial depth distribution of two selected reflectors

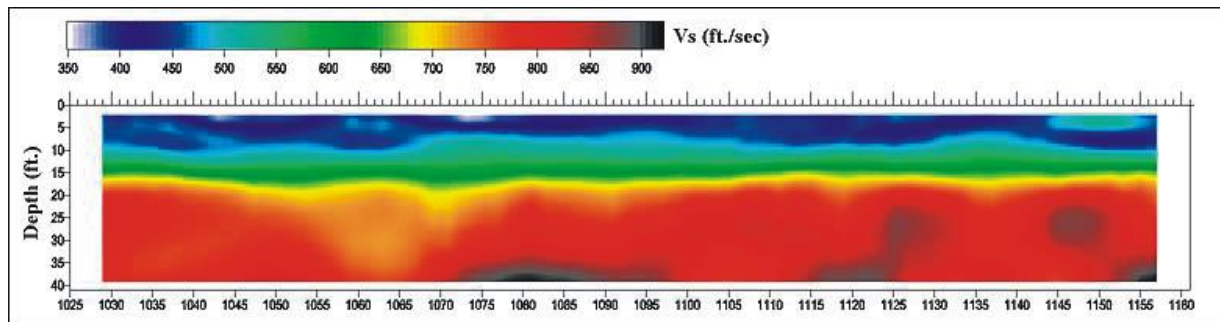
Bottom row: (left) Spatial distribution of traveltimes of a selected reflector (yellow to brown colours show the position of an anticline structure), (right) spatial distribution of the reflection amplitudes (high amplitudes can be typical for gas reservoirs)

E.8 Surface wave seismics

Surface waves are not useless. Their penetration depth is proportional to their wavelength. Velocity usually increases with depth and therefore higher-wavelength surface waves travel faster. From the dispersion analysis of surface waves (velocities of different fractions of surface waves, i.e. with different wavelengths) one gets an imaging of the velocities (shear wave velocities v_s as the velocity of surface waves is related to v_s).



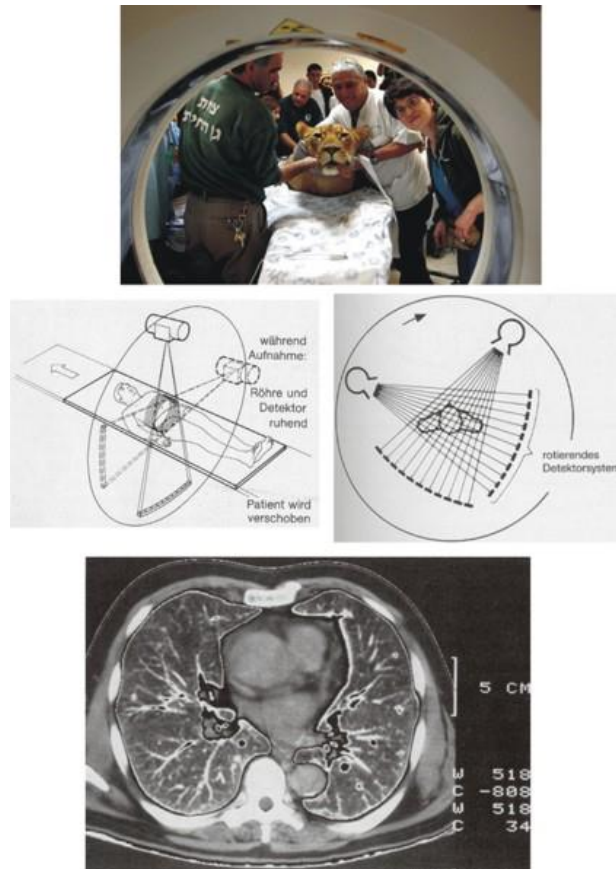
Velocity model for the propagation of surface waves (Knödel et al., 1997)



Results of a surface wave survey

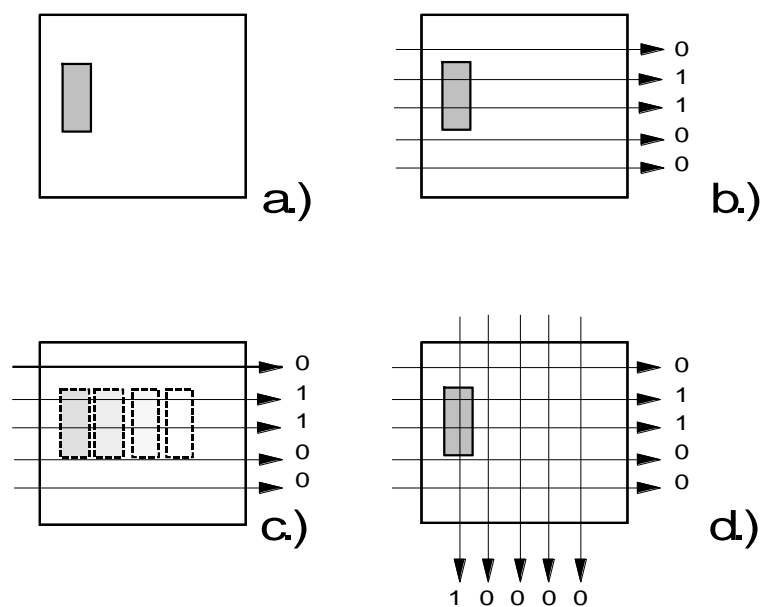
E.9 Tomography using seismic waves

(equivalent for electromagnetic waves)

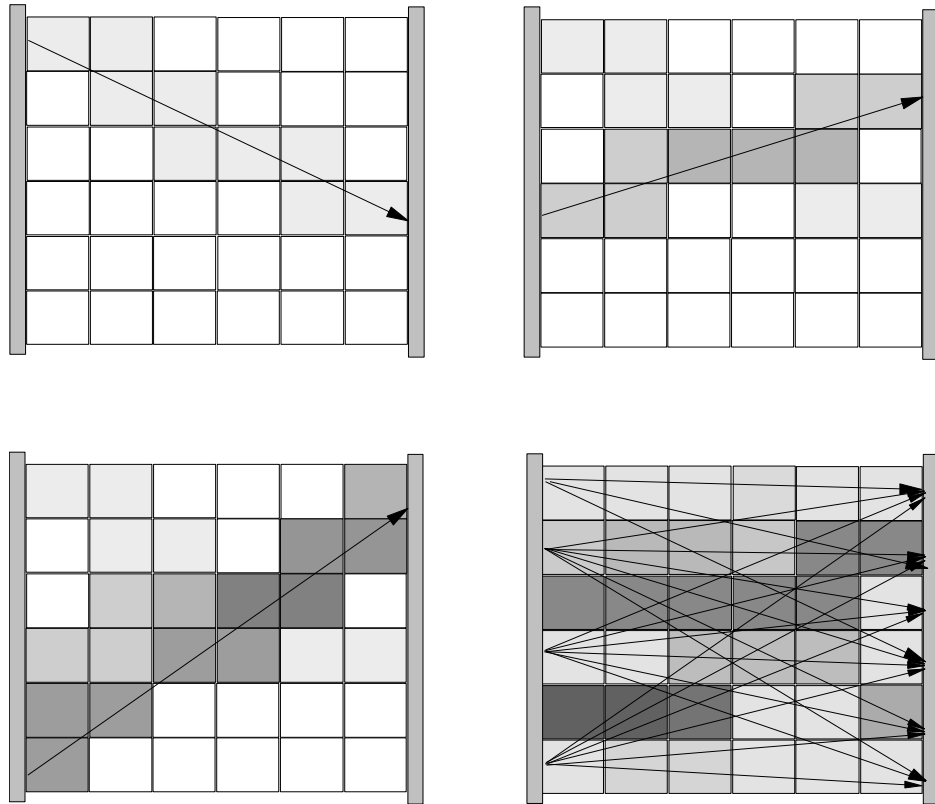


X-ray tomography for medical diagnosis (absorption is measured)

E.9.1 Concept of wave tomography

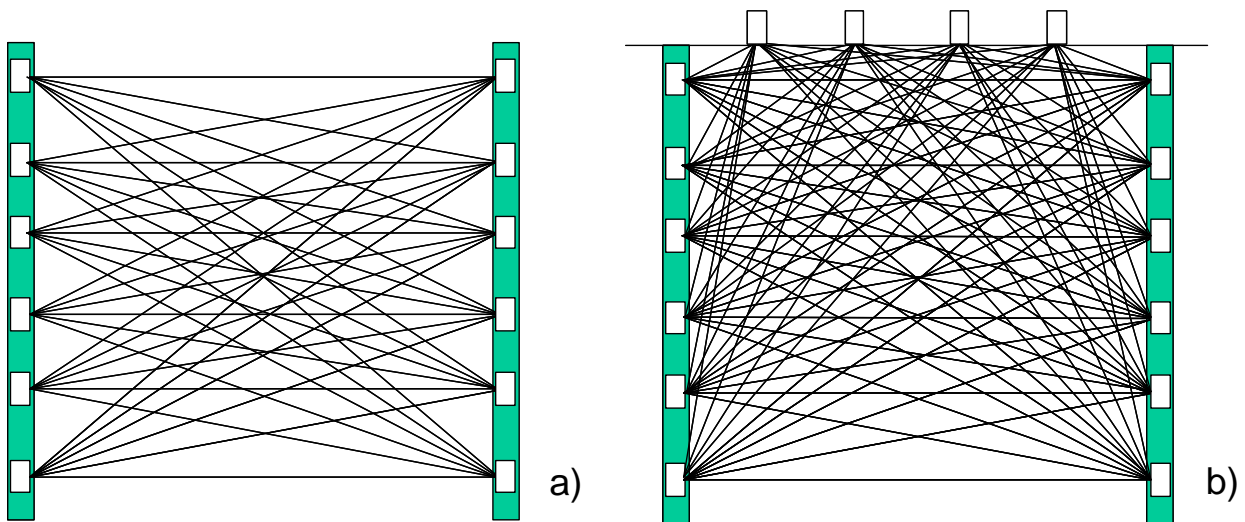


Concept of tomographic measurements

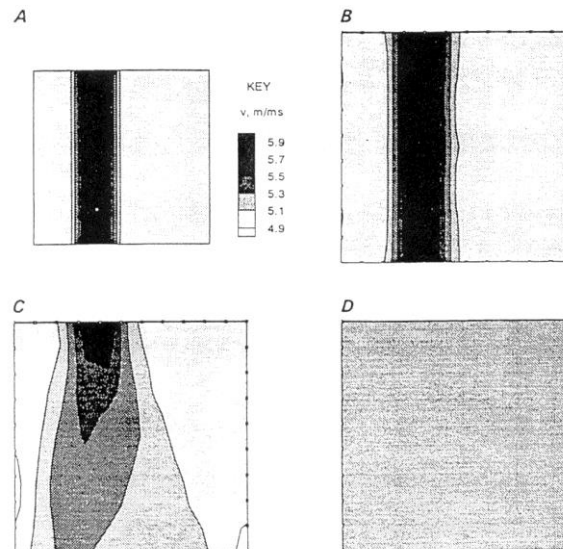


Coverage of cells by transmitted rays

E.9.2 Configurations



Configuration for tomographic measurements
cross hole (a), cross hole & hole-surface (b)



Example for the influence of ray coverage on the solution of the inverse problem of seismic tomography. A) target velocity model; B) result of reconstruction using complete ray-path coverage; C) reconstruction using data from measurements with borehole and surface instruments; D) reconstruction using cross hole data only.

E.9.3 Inversion

In seismic tomography (and also radar tomography) usually the traveltimes are measures (yielding velocity tomograms), in contrast to X-ray tomography where absorption is measured.

$$t_i = \sum_{j=1}^n s_{ij} \cdot l_j$$

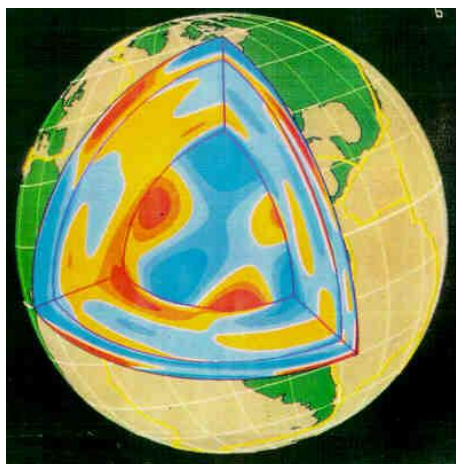
Separating the field of investigations into n cells with slowness $l_j = 1/v_j$ (v : velocity)

Traveltimes of m rays are measured (t_i)

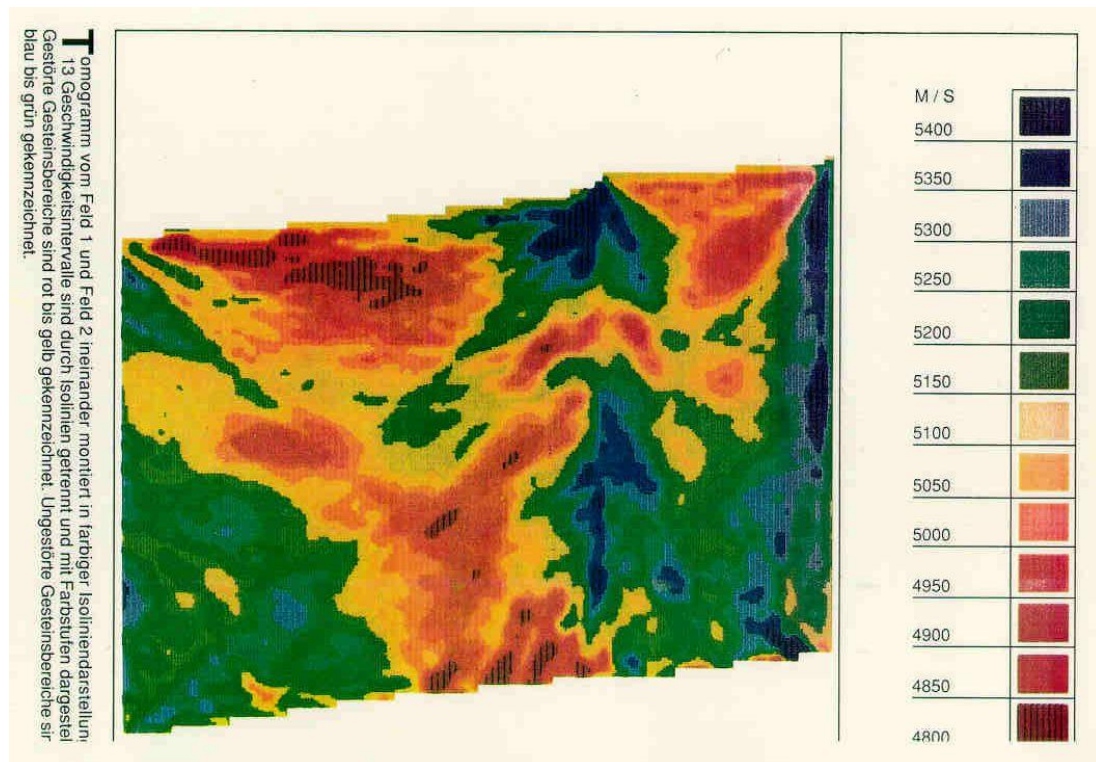
s_{ij} : ray path length of i -th ray through j -th cell

Inversion is done by an iterative process

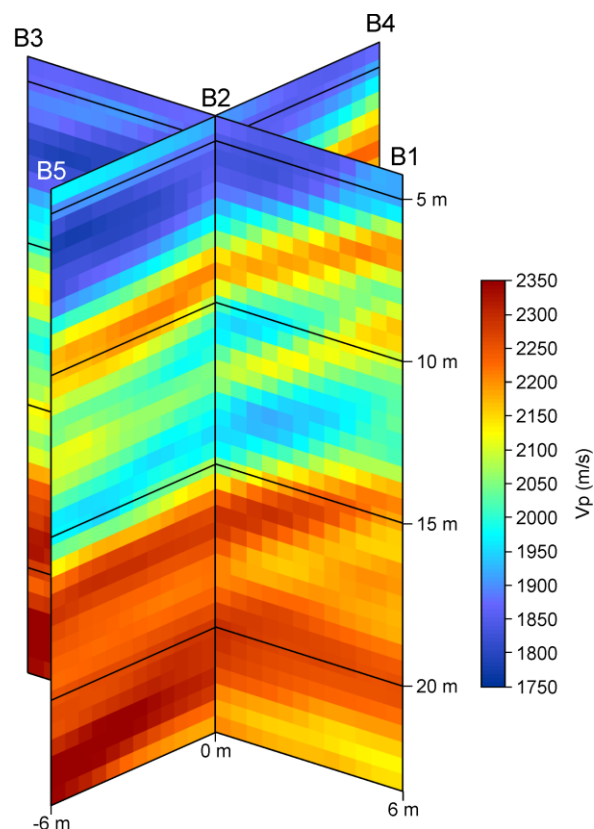
E.9.4 Examples



Tomogram of the Earth's interior (blue/red: higher/lower velocities compared to average).



Tomogram of a granite: Measurement between galleries in distances of several hundred meters.

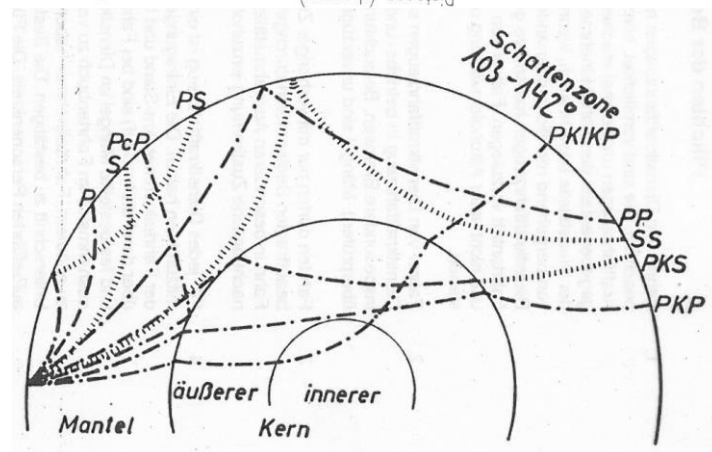
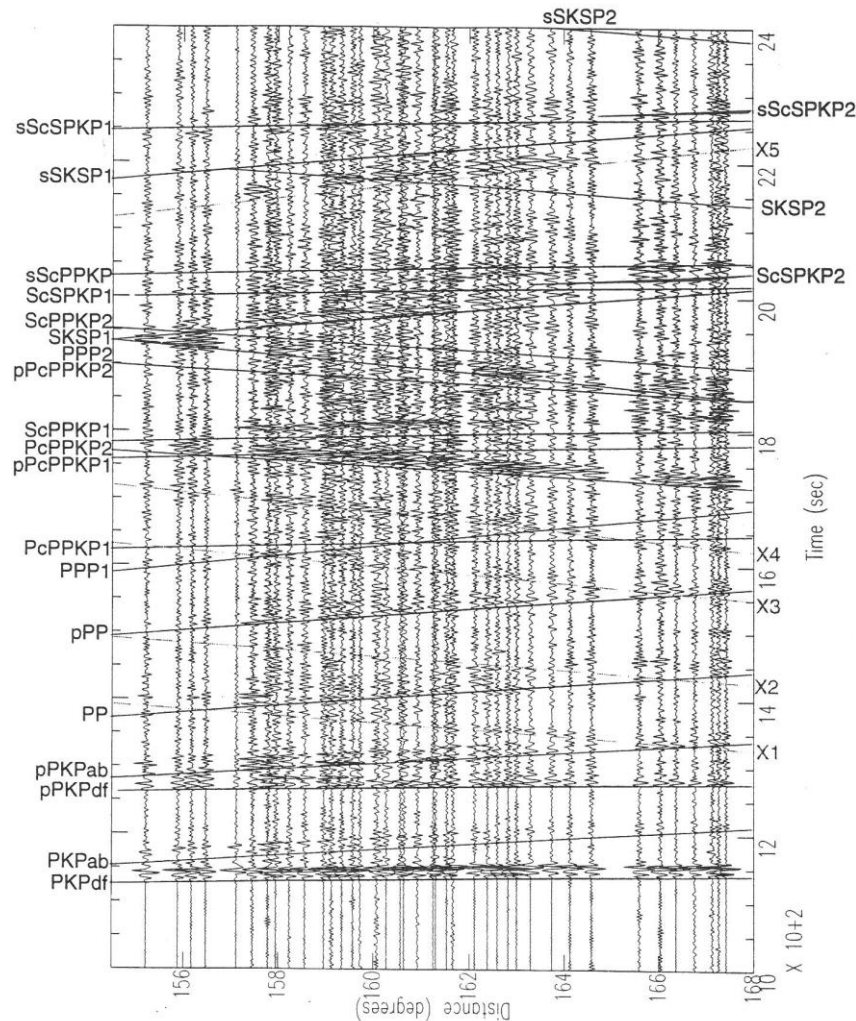


Tomogram of unconsolidated sediments: Measurement between boreholes.

E.10 Seismology (earthquakes)

E.10.1 Earthquake seismograms and the Earth's interior

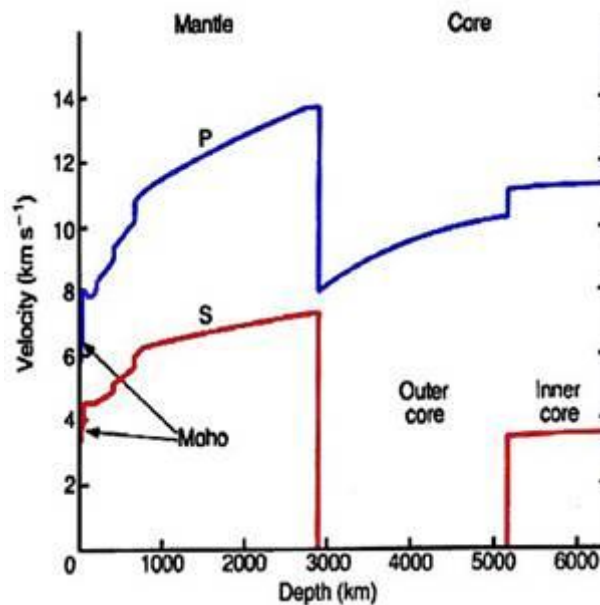
Earthquakes are regularly recorded by seismological stations and monitored at world data centres. Due to the different travel time paths through the Earth earthquake seismograms are long and complex (see figure in E.10.5).



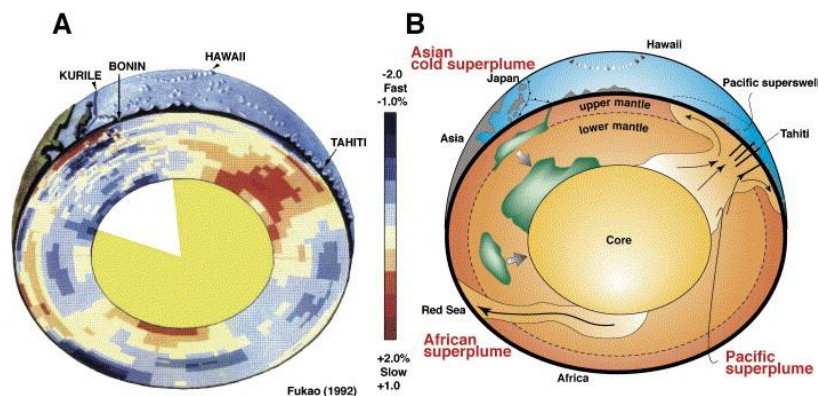
Seismic waves through the Earth's interior

P - P wave, S - S-wave; K & IK – travelled through the outer / inner core; c – reflected at the core boundary

Earthquake seismograms have provided our insight into the structure of the Earth's interior.



Velocities of P and S waves versus depth.



Tomographic results of earthquake seismograms

Blue / red colours show zones with higher / lower velocity than average at that depths, related to relatively colder / warmer temperature and interpreted as down-welling / up-welling convections

E.10.2 Focal time and epicentre / hypocentre

Focal time t_0 : time when the earthquake started (mostly given in UTC: coordinated universal time)

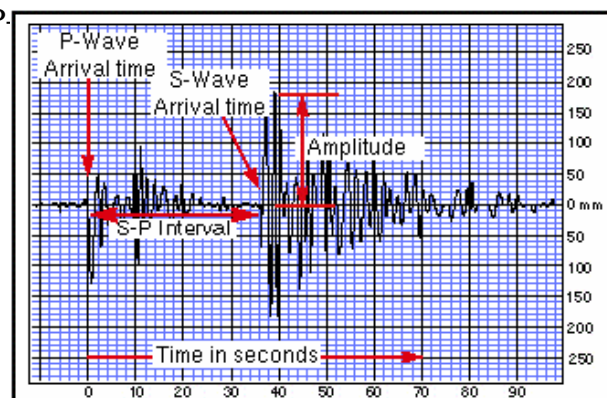
Hypocentre: location where the rupture occurred

Epicentre: location at surface vertically above the hypocentre

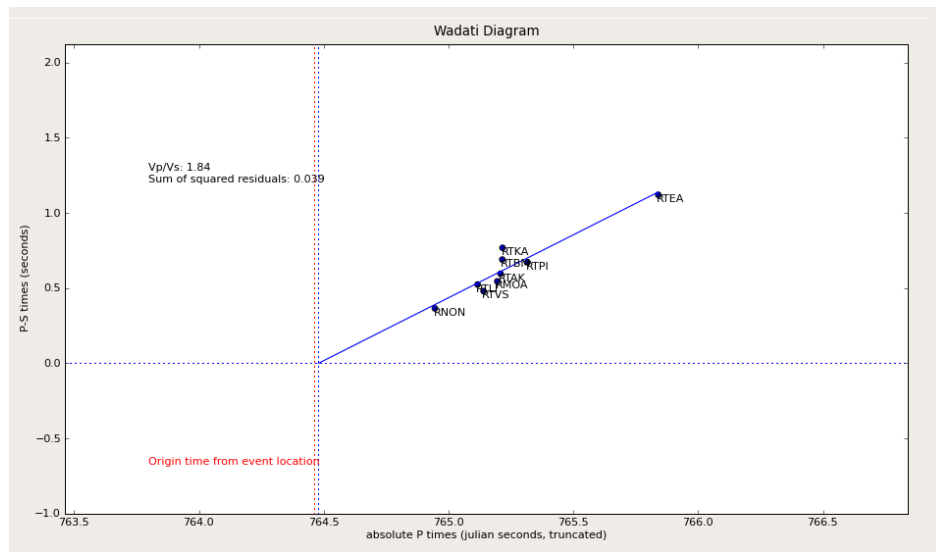
The delay time of the S-wave in respect to the P-wave is a measure of the distance s from the hypocentre to the monitoring station (in the example $t_s - t_p$ is 36 s).

$$t_s - t_p = \frac{s}{v_s} - \frac{s}{v_p} = \frac{s}{v_p} \left(\frac{v_p}{v_s} - 1 \right) = (t_p - t_0) \left(\frac{v_p}{v_s} - 1 \right)$$

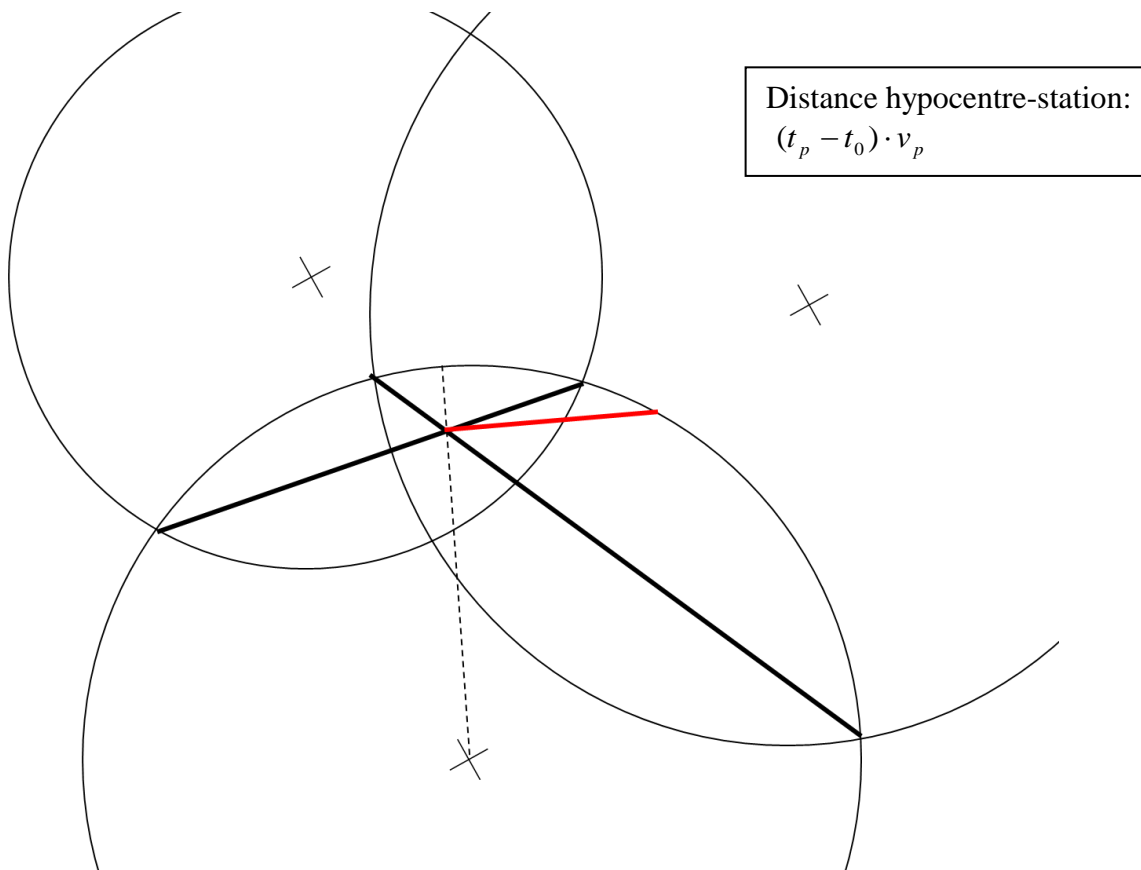
(t_s and t_p are arrival times in UTC)



The **focal time** (in UTC) can be determined by extrapolating $t_s - t_p$ versus t_p (in UTC) to $t_s - t_p = 0$.



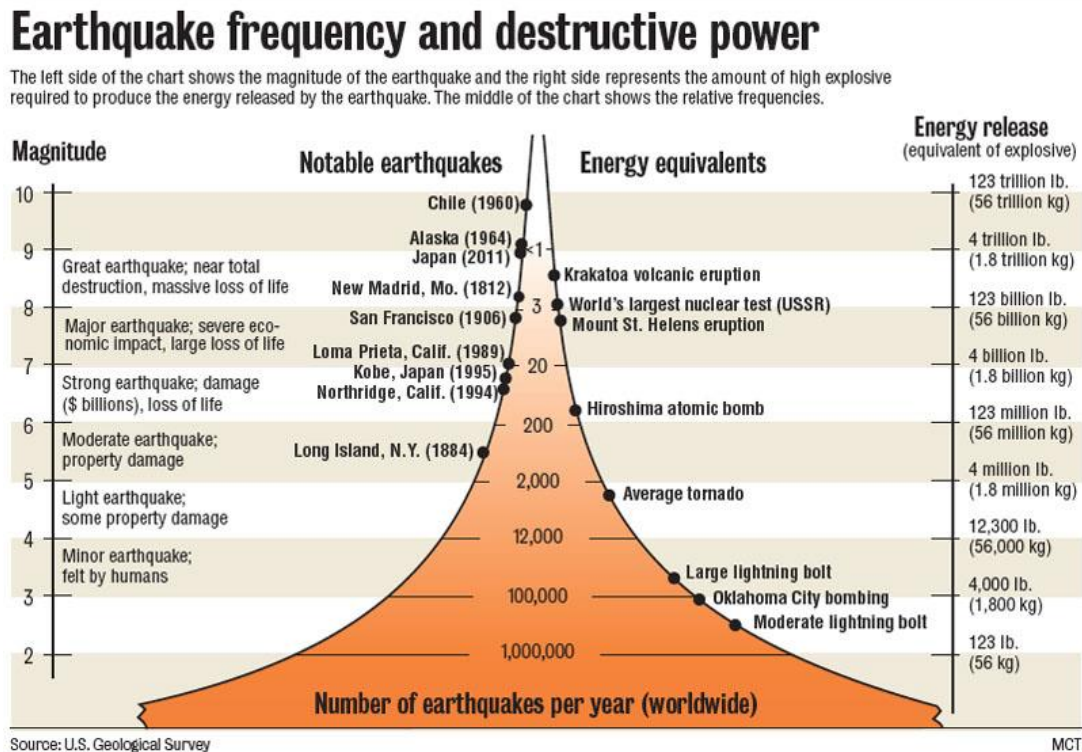
The **epicentre** and **hypocentre** can be determined from the distances between the hypocentre and the stations (minimum three stations required); the distances are known after the focal time has been determined.



Determination of the epicentre and hypocentre: The figure shows a surface projection. Crosses are seismological stations. Half-spheres (circles in this projection) around stations with a radius equivalent to the hypocentre-station distance are possible hypocentre locations. The intersection of two half-spheres is a circle segment. The bold black lines are surface projections of such circle segments (two of the three possible ones shown here); the intersection of these lines gives the epicentre location. The hypocentre is below the epicentre, the red line is the hypocentre depth.

E.10.3 Magnitude of earthquakes

Magnitude is an approximate measure for the energy released by an earthquake ('Intensity' as e.g. classified by the Mercalli scale considers the earthquake damage). It is a logarithmic scale; one magnitude difference is equal to an ca. 32-fold energy difference (two magnitudes difference equals to 1000-fold different energy; magnitude 8 equals to ca. 10^{17} J).



There are several magnitude definitions that developed historically:

The **local magnitude** M_L is the original Richter scale (developed by C.F. Richter in 1935 for classifying earthquakes in California):

$$M_L = \log A_0; \text{ amplitude } A_0 \text{ on a Wood-Anderson seismograph (measures ground motion)}$$

An amplitude of $A_0=1$ mm for epicentre in 100 km distance gives $M_L=3$.

This magnitude definition is only valid for distances to the hypocentre of ca. <600 km and magnitudes up to ca. $M_L=6.5$, strictly seen only for the subsurface conditions of California.

The **body wave magnitude** m_b and **surface wave magnitude** M_s were introduced to classify stronger earthquakes and to use seismograms recorded at far-distant stations. Both scales use the ratio A_0/T (A_0 : amplitude, T : period) that is a measure of the ground velocity.

$$m_b = \log \frac{A_0}{T} + Q(\Delta, h); \quad M_s = \log \frac{A_0}{T} + 1.66 \log \Delta + 3.3; \quad \text{insert } A_0 \text{ in } \mu\text{m}, T \text{ in s}, \Delta \text{ in } ^\circ$$

Both use the largest signals in the seismogram for body waves in the period range of 1-5 s and surface waves of T at ca. 20 s. Q is a term between ca. 6-8 depending on the epicentre distance Δ (angle of the sector between the epicentre and the station seen from the Earth's centre) and the depth h of the hypocentre (Q can be determined from charts). Above a magnitude of ca. 8, both m_b and M_s clearly underestimate the true strength of earthquakes.

Only for a magnitude between ca. 6 to 6.5, the above magnitude scales give the same value.

M_L , m_b and M_S only use the strongest signals in the seismogram. Because of this and other limitations the more general **moment magnitude M_W** was developed that is nowadays commonly applied. M_W can be determined from analysing the whole seismogram. There is a relationship with the seismic moment M_0 :

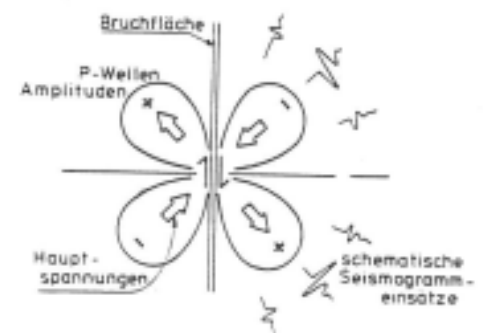
$$M_W = (2/3)(\log M_0 - 9.1) \quad (M_0 \text{ in Nm})$$

$$M_0 = \mu \cdot F \cdot d$$

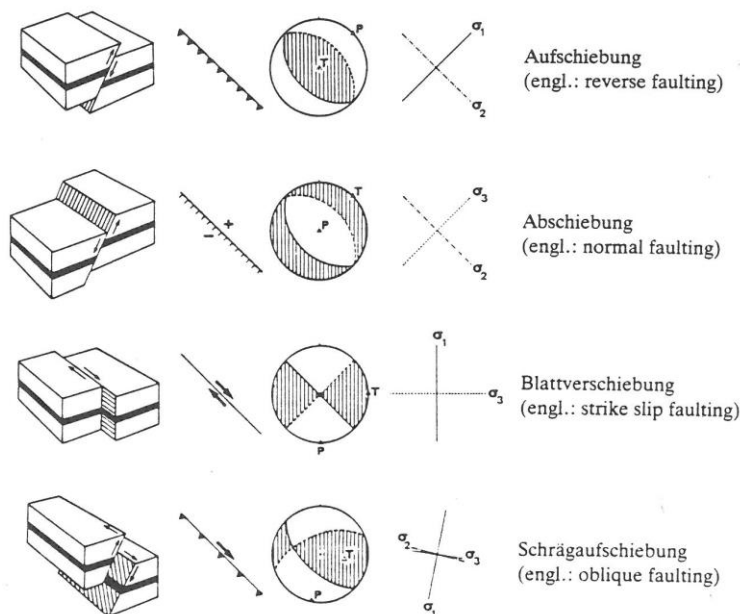
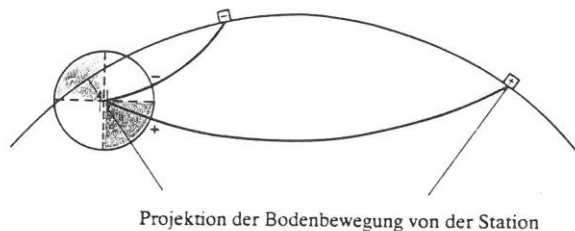
μ : shear modulus; F : ruptured fault area; d : displacement on the fault

E.10.4 Fault plane solutions

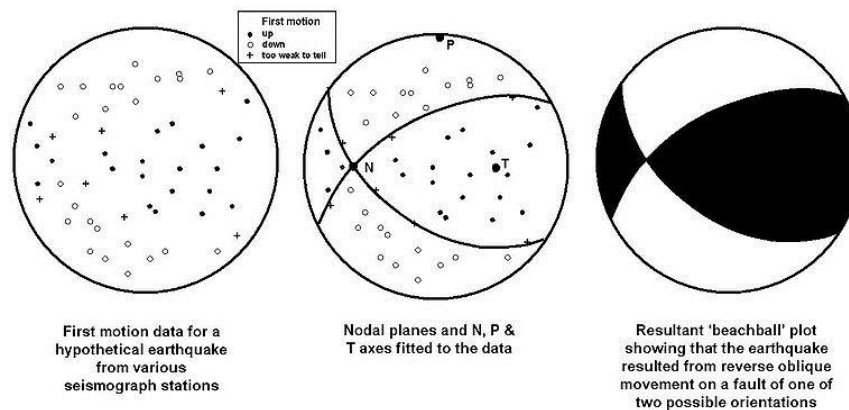
Fault plane solutions are lower hemisphere projections of first compressional and dilatational seismic signals emerging from the hypocentre. The directions of first compressional signals are illustrated in black, first dilatational signals in white. Fault plane solutions relate seismic signals to the tectonic displacement (note: there always two possible displacement directions resulting from a given fault plane solution).



Stress at a fault and seismic waves created by rupture



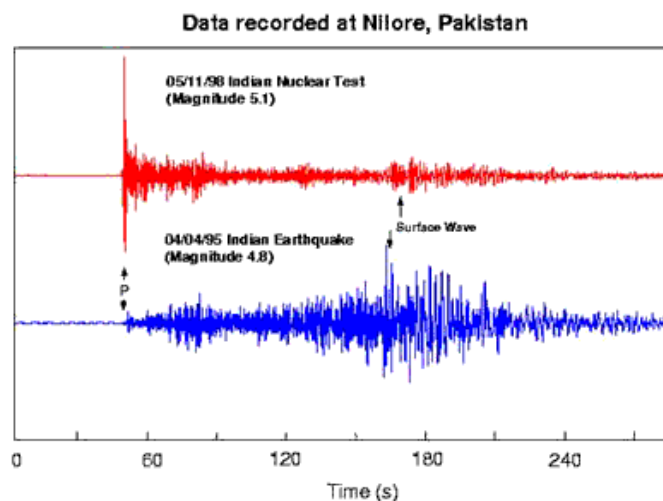
Principle of fault plane solutions: first seismic signals in up and down directions (corresponding to first movements away from and towards the hypocentre, respectively) come from compressional/dilatational zones.



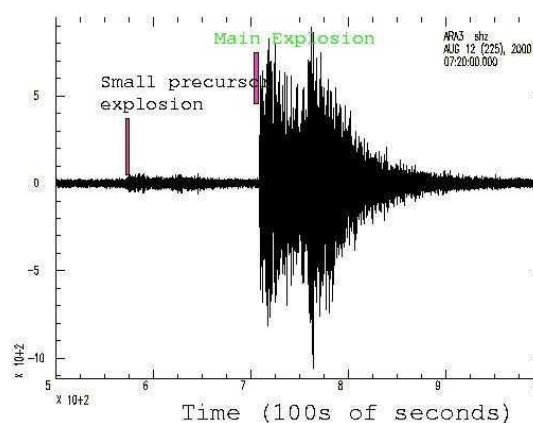
Construction of a fault plane solution from seismic signals (each point in the projection refers to one seismic station)

E.10.5 Distinguishing earthquakes and explosions

Distinguishing in between earthquakes and explosions has a practical application in monitoring the nuclear test ban treaty. Earthquakes show a major contribution of both P-waves and S-waves, while explosions mainly show P-waves but little S-waves and surface waves signals.



Comparison of seismograms of the 1998 Indian nuclear test with an earthquake in India of ca. the same strength

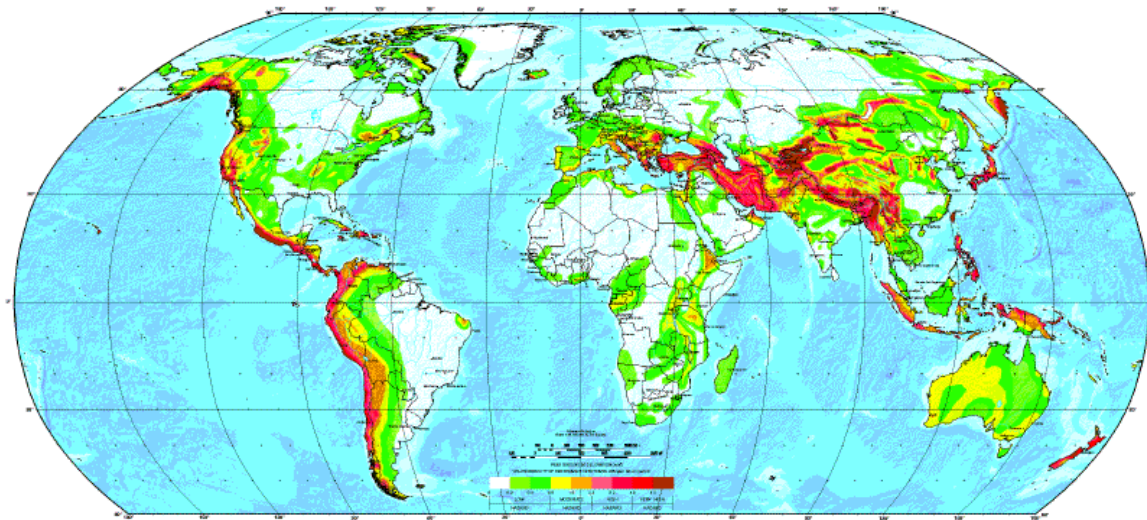


The tragic sinking of the Russian submarine Kursk on 12th August 2000 in the Barents Sea recorded at a seismological station in northern Norway (two explosions within ca. two minutes are seen)

E.10.6 Seismic hazards (zones of high-magnitude earthquake risks)

With our present knowledge we can outline risk areas for potential strong earthquakes. These are related to subduction zones, 'young' continental collision zones and strike-slip faults. There is no reliable possibility for short-term prediction of earthquakes. Earthquake recurrence intervals, 'seismic gaps' and earthquake precursors were intensively studied but did not result in a common understanding of their use in predicting earthquake events.

GLOBAL SEISMIC HAZARD MAP



Seismic hazard map of the Munich RE

Geophysical Text Books

(German)

Clauser: Einführung in die Geophysik: Globale physikalische Felder und Prozesse in der Erde, ca. 420 p.

Springer

Bender (Hrsg.): Angewandte Geowissenschaften Bd.II: Methoden der Angewandten Geophysik und mathematische Verfahren in d. Geowissenschaften, ca. 750 p.

Enke

Militzer, Weber: Angewandte Geophysik, 3 Bände, je ca. 350-400 p.

Springer

Knödel, Krummel, Lange: Geophysik. Bundesanstalt für Geowissenschaften und Rohstoffe (BGR) - Handbuch zur Erkundung des Untergrundes von Deponien und Altlasten, Bd. 3, ca. 1040 p.

Springer

(English)

Telford, Geldart, Sheriff: Applied Geophysics, ca. 750 p.

Cambridge University Press

Sharma: Environmental and Engineering Geophysics, ca. 470 p.

Cambridge University Press

Lowrie: Fundamentals of Geophysics, ca. 340 p.

Cambridge University Press

Robinson, Coruh: Basic Exploration Geophysics, ca. 540 p.

John Wiley & Sons

Griffiths, King: Applied Geophysics for Geologists & Engineers, ca. 220 p.

Pergamon Press